INTERNATIONAL ATOMIC ENERGY AGENCY
UNITED NATIONS EDUCATIONAL, SCIENTIFIC AND CULTURAL ORGANIZATION
INTERNATIONAL CENTRE FOR THEORETICAL PHYSICS
I.C.T.P., P.O. BOX 586, 34100 TRIESTE, ITALY. CABLE: CENTRATOM TRIESTE

SMR.755/16

Workshop on Fluid Mechanics

(7 - 25 March 1994)

Northern and southern hemisphere seasonal variability of blocking frequency and predictability

E. Tosi
S. Tibaldi
A. Navarra
L. Pedulli

NORTHERN AND SOUTHERN HEMISPHERE SEASONAL VARIABILITY OF BLOCKING FREQUENCY AND PREDICTABILITY

S. Tibaldi, E. Tosi, A. Navarra(*) and L. Pedulli

University of Bologna, Department of Physics
Atmospheric Dynamics Group
Via Irnerio 46, I-40126 Bologna, Italy

Submitted to Monthly Weather Review, May 1993
Revised Version, December 1993

(*) CNR-IMGA, Via Emilia Est 770, I-41138 Modena, Italy

Abstract

Seven years of analyses and forecasts from the operational archives of the European Centre for Medium Range Weather Forecast (ECMWF) have been analyzed to assess the performance of the model in forecasting blocking events. This paper extends the previous work by Tibaldi and Molteni (1990) to the other seasons of the year and to the Southern Hemisphere. The data set covers the period from December 1st, 1980, to November 30th, 1987, and consists of 500 hPa geopotential height daily analyses and of the ten corresponding forecasts verifying on the same day, a data set commonly known as the "Lorenz Files". Local blocking and sector blocking have been defined as in Tibaldi and Molteni (1990), using a modified version of the Lejenas and Økland (1983) objective blocking index.

The results broadly confirm the conclusions previously reached for the Winter season alone, extending their validity to the rest of the year and, *mutatis mutandis*, to the other hemisphere. The main observational difference between blocking in the two hemispheres is in the number of preferred locations: Atlantic and Pacific blocking in the Northern Hemisphere, and only one broad region in the Southern Hemisphere, around 180°E. Forecasting the onset of blocking events is in general a task that the model finds difficult whereas, if the integration starts from an already blocked initial condition, the performance of the model is usually better. The poor observational data coverage in the Southern Hemisphere is likely to produce initial conditions affected by larger errors, making the correct forecast of the onset of a blocking event an even more difficult task than it is in the Northern Hemisphere. In the Northern Hemisphere, though the dynamical characteristics of Atlantic and Pacific blocks are inferred from the respective model errors to be different, their detrimental effect on forecast performance are similar in the two cases.

1. Introduction

Despite major advances in operational medium-range numerical weather predictions, forecasting errors produced by numerical models still appear to be an important manifestation of model inadequacies. These are the sum of a "random" component and of a systematic part, the so-called climate drift (eg. Arpe, 1990 and Tibaldi et al., 1991 and references therein). Such errors are known to be synoptically related to the prevailing weather type (grossvetterlage) and Tibaldi and Molteni (1990, hereafter referred to as TM) have investigated the relationship between model behaviour (and therefore errors) and blocking in the Winter season of the Northern Hemisphere, using ECMWF operational archives of analyses and forecasts. They essentially documented the inability of the ECMWF model to properly forecast blocking onset beyond a few forecast days, and how this reflected in fewer blocking episodes being simulated by the model than in the real atmosphere.

This inability shown by forecasting models to enter into a blocked state are limiting factors of paramount importance also for the extended range forecasts (Tracton et al, 1989; Tracton, 1990; Miyakoda and Sirutis, 1990; Brankovic and Ferranti, 1992), where the consequences of such errors are amplified by the longer integration time. An improved understanding of the relationship between blocking forecast failures and model formulation and errors would therefore have an even larger impact on extended range dynamical forecasts.

In this study, the analysis on blocking operational predictability performed in TM for the Winter season of the Northern Hemisphere (NH) will, be extended to the other seasons of the year and then to the Southern Hemisphere (SH). The data used are ECMWF analyses and forecasts of 500 Hpa geopotential height fields from 1980 to 1987. The reader interested in a more up-to-date analysis of the ability of the ECMWF operational model to forecast blocking (in the Northern Hemisphere Winter only) and in particular to a quantitative evaluation of the recent improvements is referred to Tibaldi et al. (1993). Additionally, Tibaldi (1993) contains a brief account of the potentials of blocking diagnostics as a tool to assess Climate GCMs performances.

The organization of the data set and the analysis procedures are described in Section 2. Section 3 is devoted to the description of NH blocking frequency and its longitudinal variations both in observations and forecasts. Sections 4 and 5 describe the model's ability to represent blocking, with particular attention to onset and duration. Section 6 analyzes the possible effects of blocking on objective forecast skillscores. Section 7 is devoted to a separate analysis of observed and predicted blocking in the Southern Hemisphere. A summary and conclusions are contained in Section 8.

2. Description of the data set and of the analysis procedure

The database for this study consists of daily 500 hPa geopotential heights analyses and the corresponding day 1 to day 10 forecasts. For each day, eleven fields are then available: analysis and day one to day ten forecasts, all verifying on the same day but

started from progressively lagging initial conditions. Such an arrangement of analysis and forecast fields is commonly known as a "Lorenz files" dataset. The total record includes seven complete years, from December 1st, 1980 to November 30, 1987. Seasons have been defined somewhat arbitrarily as 90 day periods, the NH Winter covering the 90 days starting on December 1st (December, January and February, DJF), NH Spring from March 1st (MAM), NH Summer from June 1st (JJA), and NH Autumn from September 1st (SON). Since there are eleven records relative to each day, the complete dataset consists of 2800 days. A buffer zone of ten days is added at the end of each 90 day season to allow for blocking events straddling across seasons. The original data consisted of global fields, projected on spherical harmonics coefficients truncated at triangular truncation 40 (T40). For the present analysis the data have been projected on a regular latitude-longitude grid (3.75° × 3.75°) and only the regions North of 20°N for the Northern Hemisphere and South of 20°S for the Southern Hemisphere have been considered.

The ECMWF operational data assimilation scheme and forecasting model have constantly been modified during the seven-year period under consideration. Changes have been as major as a complete revision of the physical parametrizations, and the transformation from grid point to spectral numerical schemes. TM considered the problem of the impact of these modifications on the representation of blocking in the Northern Hemisphere Winter, performing the diagnostic analysis separately for the different periods in which the model was not changed, and their conclusion was that the model development during these seven years did indeed produce some improvement of the ability "to represent blocking at an advanced state during the forecast". This impact, however, was found not to be substantial. Recently, Tibaldi et al (1993) have shown that the operational model has indeed measurably improved its performance in Winter during the most recent years.

A local and instantaneous blocking index, based on the TM modification of the original index by Lejenas and Økland (1983), will be used throughout this work. The index and the blocking criteria are extensively discussed in TM, therefore only a brief definition, for sake of completeness, will be given here. For the Northern Hemisphere (the modifications necessary to apply the index in the Southern Hemisphere will be discussed in Section 7) two values of the geopotential height gradient are evaluated at each longitude:

$$GHGS = z(\phi_0) - z(\phi_s)/(\phi_0 - \phi_s) \quad (2.1)$$

$$GHGN = z(\phi_n) - z(\phi_0)/(\phi_n - \phi_0) \quad (2.2)$$

where

$\phi_n = 80°N + \Delta$
$\phi_0 = 60°N + \Delta$
$\phi_s = 40°N + \Delta$

and $\Delta = -3.75°, 0°, +3.75°$.

A given longitude is then defined to be blocked at a certain instant in time if the following conditions are both satisfied for at least one of the three values of Δ:

$$GHGS > 0 \quad (2.3)$$

$$GHGN < -10 \text{ m/(° latitude)} \quad (2.4)$$

Condition (2.4) was added by TM to the original Lejenäs and Økland index, i.e. condition (2.3 alone), to ensure that cut-off lows anomalously displaced to the North were not counted as blocks.

This criterion is different from other objective definitions of blocking to be found in the literature (e.g., Dole and Gordon, 1983; Lau, 1983), but satisfies the requirements of time and space locality useful in this type of analysis. However, a local and instantaneous index such as this is capable to identify blocking-like structures, but has to be supplemented by further conditions, reflecting the synoptic requirements of spatial extension and time duration, which distinguish a transient blocking-like flow pattern from a true blocking event. Such conditions will be developed and added in the forthcoming section, where the concept of blocked sector will be introduced. Lejenas and Økland (1983) and Ruti (1992) have shown that the index is quite consistent with synoptic assessments of blocking events. Moreover, the main objective of this paper is to perform a relative comparison between observations and forecasts, and therefore the detailed nature of the blocking indicator should not affect the major conclusions of the work.

3. Northern Hemisphere observed blocking patterns, frequency and distribution

The results of the computation of the simple blocking local index on the complete observational database in the Northern Hemisphere is shown in Fig. 1. The top panels (a to d) show the observed percentage frequency of blocking as a function of longitude for the four different seasons. The quadrants of preferred Winter blocking are well evident in panel 1a and correspond to the synoptically known Euro-Atlantic (EA) and Pacific (PAC) blocking regions, separated by two gaps around 100°E and 255°E, where the circulation flow appears to be predominantly zonal, according to the index. A minor maximum can also be detected between 50°E and 70°E, but it is difficult to separate it clearly from the major adjacent EA peak. The two major blocking peaks reach a similar maximum value of approximately 20%, indicating that Winter blocking has an approximately equal frequency of occurrence in the two Pacific and Euro-Atlantic sectors.

These two major blocking features persist through Spring. The EA maximum blocking frequency increases up to 25% and shifts from around 15°E to 30°E whereas the Pacific peak weakens considerably, reducing its maximum amplitude to about one half of its Winter value. An even deeper gap separates the peaks at around 90°E, while the Great Plains separation at around 250°E is lifted somewhat.

The picture is different in Summer. The EA blocking feature has lost coherence and strength, the previous strong peak being broken into many weaker features, amongst which it is difficult to identify a coherent structure. The central Asian gap (around 90°E) is harder to distinguish and a noisier distribution appears in that area, while the gap over the Great Plains and the North American continent is now more evident. The Pacific area shows little difference with respect to the Spring situation. The previous distinctive Winter pattern appears now in disarray to the point that a clear definition of EA and PAC blocking areas would be impossible based on the data of this season alone.

Although Autumn is the season showing the lower overall blocking frequency, during this period the EA peak starts rebuilding, while the PAC sector is almost completely quiescent.

The strong geographical localization, particularly evident in Winter and Spring, together with the arguments on the nature of the objective index introduced at the end of section 2, suggest that an analysis based on "sectors", rather than on isolated longitudes, should be more appropriate. As in TM, two sectors are then identified, Euro-Atlantic and Pacific, with the following longitudinal limits (note that the limits of the Euro-Atlantic sector have been slightly modified with respect to TM, where they were 28° W and 32° E):

Euro-Atlantic:	22.5° W	45° E
Pacific:	152° E	136° W

A sector is then considered to be blocked if three or more adjacent longitudes within the sector are blocked according to the previous index definition. The sector definition is kept fixed for all seasons.

In addition to this criterion on spatial extension, a further constraint on duration in time is needed to approach the synoptic concept of blocking "a la Rex". This has been done by requiring, for a blocking event (or episode) to be catalogued, that a sector is blocked for at least five consecutive days. This is a totally arbitrary limit, which stems from the compromise of having true long-lasting blocking events, but also a sufficient number of them to constitute a minimal statistical base.

The results of the application of these further conditions on the observed database are collected in Table 1. The largest amount of blocked days (but also events) for the Euro-Atlantic sector occurs in Spring, whereas in the Pacific sector Winter appears to be the preferred season for blocking. The seasonal march of blocking frequency is shown in detail in Fig. 2 for both sectors. Blocking in the Northern Hemisphere is thus confirmed to be characterized by a marked seasonal cycle; in fact, EA blocking by itself would define only two extended seasons, a blocked Winter-Spring and a zonal Summer-Autumn. In the Pacific, blocking seems to be a phenomenon mostly confined to Winter, with a weak secondary peak in Summer. The seasonal cycle of both sectors appears to have higher frequency structures superimposed, with relatively isolated maxima in March and May in the EA and in September and July

for PAC. It is likely that such structures are an artifact of the limited sample of the database and of the particular definition of the blocking index.

As a mean to check the sector analysis procedure, the sector analysis was performed on the gap region evident in Fig. 1a between 70° and 130° East, which is a region where an absolute minimum of blocking episodes is to be expected. The total number of these "background" blocking events can be taken as an estimate of a threshold value above which a signal should be detectable from the background noise. This "confidence threshold limit" could be conservatively estimated at the frequency value of 15%, which means that all blocking peaks in Fig. 2 are well above this confidence level for all seasons, thereby indicating that the definition of blocked sector appears to be consistent.

In order to highlight synoptic patterns corresponding to sector blocking regimes, the following procedure has been applied. Data have been classified according to whether a day is zonal, Pacific blocked or Atlantic blocked. Days blocked in both sectors at the same time have not been singled out in a separate category (a "global blocking" regime) due to their small overall number; therefore, they appear in both blocked classes. Anomaly maps of the blocked regimes have then been constructed by compositing (i.e. ensemble averaging) the maps of the two blocked categories and subtracting out the composite of all zonal days (the "zonal" regime). Figure 3 shows NH 500 hPa mean maps of the anomalies corresponding to the two blocked regimes for the four seasons.

Figure 3 documents a noticeable yearly cycle of intensity and pattern shape of blocking signature in both the Atlantic and Pacific sectors. The Winter regime anomalies (panels a and e for Euro-Atlantic and Pacific sectors respectively) show the familiar blocking highs. Lows appear to the North and South of the main blocking high, whereas the residual high over the opposite hemispheric sector results mostly from those blocking episodes occurring at the same time over both sectors (the "global" blocks). The main feature of the Spring anomalies (panels b and f) is the relative prevalence of the Atlantic peak over the Pacific. The Atlantic signature also shows up in the Pacific blocking regime much more than in the opposite case. An examination of the time sequences of the blocking indices shows that the long duration of the Atlantic blocking episodes during Spring makes global blocking rather more probable than average. Summer and Autumn anomalies (panels c, g and d, h of Fig. 3 respectively) show similar features.

4. Short- and medium-range forecasts of blocking in the Northern Hemisphere

Before analyzing the model's ability in representing blocking, and as a preliminary measure of general model performance, we begin by showing here 500 hPa geopotential height model systematic errors, i.e. ensemble mean of forecast minus analysis fields, according to season. The results are shown in Figure 4, where it is evident that Winter is the season with the largest amplitude systematic errors. It can also be noted that the Winter systematic error of the model has a synoptic structure reminiscent of (but opposite in sign) the superposition of the synoptic structures of

Euro-Atlantic and Pacific sector blocks (Figs. 3a and 3e). Additionally, a distinctive feature of the Summer SE is the strong positive maximum in correspondence of the left-exit of the Asian jet and a rather featureless and weak negative SE elsewhere.

We now turn to the computation of the objective blocking index on all forecast fields, providing therefore a measure of model performance. A detailed analysis of the behaviour of the ECMWF operational forecasting model in Winter alone can be found in TM. That work has been extended here to the other seasons but, for reasons of brevity, comments will be restricted to some selected forecast times (mostly day 3 and day 10, respectively representative of the short and medium range) and to a selection of diagnostic quantities.

In the middle and bottom panels of Fig. 1 (e to h and i to l), the longitude dependence of the local blocking index for the forecasts at day 3 and day 10 is shown, together with the corresponding verification diagram (dotted). The forecasts appear to underestimate the frequency of blocking days in all seasons and for all forecast times, with the possible exception of short range forecasts during Autumn (September to November). This effect appears to increase with increasing forecast time, with the underestimation already evident at day 3 and well evident at day 10. A further analysis of the number of correctly predicted blocked days versus forecast time (Figures 5 and 6, respectively for EA and PAC sectors) reveals that the decrease of correctly predicted blocked days is, regardless of the season, very fast (in some seasons/sectors almost linear, but in the worse cases approximately exponential), confirming the results of Miyakoda and Sirutis (1990) who found a similar behaviour of blocking forecast skill in a study concerning a number of 30 days forecasts with the GFDL model.

Turning now to sector diagnostics, we can assume the maximum value of the quantity GHGS (equation 2.1, section 2) inside the blocked sector as an estimate of the intensity of the block, and the longitude at which this maximum is attained as an estimate of the phase. It is then possible to derive some more precise quantitative assessment of the model behaviour and performance as a function of forecast time. Fig. 7 shows, season by season (panels a to d), the error in blocking intensity (difference between the maximum value of GHGS computed over the observed and forecasted fields) as a function of forecasting time averaged over all correctly predicted blocking episodes in each sector. There is a general tendency to underestimate blocking intensity, modulated by a large seasonal variability of the model behaviour. The exception is provided by EA blocking during Autumn, for which the intensity is overestimated up to forecast day 6. Spring seems to provide the overall best model performances in forecasting blocking intensity, both for the Atlantic and the Pacific sectors, while extreme seasons (Winter and Summer) both show a similar behaviour, with PAC blocking being ill-treated by the model more than its EA counterpart well into the medium range.

Phase errors (differences in the longitude of the maximum value of GHGS between analysis and forecasts) are shown in Fig. 8. Large drifts of opposite signs increasing throughout the forecast time are evident in Winter and Summer, corresponding to a systematic model eastward shift of Atlantic blocks and westward shift of Pacific

blocks. Phase errors seem to be negligible in comparison during transition seasons, confirming the comparatively better skill of the model in these seasons already evident in the blocking intensity diagrams of Fig. 7. Since these are mean (systematic) errors, a degree of cancellation between positive and negative errors is taking place. RMS errors of both phase and amplitude (not shown) are approximately 40% to 50% larger than their corresponding mean values.

The large fluctuations evident in forecast errors of both blocking intensity and phase from forecast days 4 and 5 onward are most likely due to the progressively decreasing number of correctly predicted blocks as forecast time increases, which in turn impoverishes the sample on which forecast errors are computed. The importance of this fact will become even more evident in the next section.

5. NH Blocking onset and blocking duration

It is commonly accepted that forecasting blocking onset is a difficult task for operational prediction models (e.g. Grønas, 1983). The instability nature of the process of entering the blocking state, which has often been advocated in theoretical blocking studies, would in fact justify such difficulties, but on the one hand the precise physical nature of the instability process has never been satisfactorily and uniquely (if possible) identified; on the other hand, precise quantitative evidence of the above-mentioned forecasting difficulty has only recently started to be brought forward (e.g., TM, Tracton et al, 1989 and Miyakoda and Sirutis, 1990). It appears therefore useful to try to quantify such difficulties and their dependence upon seasons.

Blocking onset is therefore defined as the transition between a zonal day and a blocked day in a given sector and it becomes possible to verify how far back in time it is possible to go before the ability of modelling such a transition as an initial value problem vanishes. Figure 9 attempts to do just this for the Euro-Atlantic sector: each blocking episode is represented by a column. In each column, a black square indicates that the forecast started n days (n being the value along the y-axis of each panel) before the onset date of the event (the first blocked day) was blocked, and a hollow square that it was not. Day 0, being the analysis, is obviously indicated as blocked for all cases. The total number of blocking episodes in each season (the number of columns in each of the four panels) corresponds to the numbers indicated in the third column of Table 1. The episodes are ordered chronologically along the x-axis and columns are grouped in sub-sets to indicate that they took place in the same year. There are usually seven sub-sets in each panel, as many as the number of years in the dataset. If they are less than seven (e.g. Pacific blocking in Spring), this indicates that there are years with no blocking episodes in a given season.

The model displays, in the EA sector, a large case-to-case variability of skill, composed of both intraseasonal and interannual contributions, but no clear systematic seasonal cycle or secular trend are apparent. Good and bad cases appear to be fairly uniformly scattered throughout the seasons and the years. The situation for the Pacific sector, shown in the companion Figure 10, is also rather similar, with no apparent trends well evident.

Figures 11 and 12 try to give a summary of this information by counting the total number of successful blocking onset forecasts as a function of forecast time. There is an approximately exponential decrease in the number of correctly predicted onset in both the Atlantic and the Pacific sectors. The decrease appears to be more rapid in Winter and less so in Spring. About 50% of the onset are correctly forecasted four days ahead in Spring, but only 30% in Winter, and 14% in Summer. Similarly, for the Pacific case, about 40% of the cases are forecasted correctly four days ahead in Winter and 25% in Summer, the two seasons containing, in this sector, the largest number of cases.

We now turn our attention to blocking maintenance, that is the ability of the model at predicting blocking duration. This is shown in Figures 13 and 14. We restrict here the analysis to those forecast starting on the very first day of the blocking event, i.e. containing the blocking already in the initial conditions. In the two figures, black and white bars represent respectively the duration of the observed blocking event in the analysis and in the forecast. Bars (events) with a white top indicate a forecast of a blocking episode longer than observed, while bars with a black top indicate the opposite. Correct forecasts, as far as blocking duration is concerned, are indicated as completely black bars. Events which last longer than ten days are grouped together and indicated as eleven-days events.

The overall model performance is good and a number of outstanding successes with relatively long-lasting blocks are apparent. Furthermore, the model appears to be measurably more successful at predicting the correct duration of Euro-Atlantic blocks than of Pacific blocks, although this difference is probably statistically not significant, due to the limited sample of events. A quantitative evaluation of the statistical significance of the difference between the RMS error of blocking duration in the two sectors is made very difficult by the large number of blocks with duration longer than ten days, for which computing a duration error is not possible. However, histograms of blocking events duration can be computed to verify the qualitative impression (Figs. 15 and 16). It is possible to note that long (> 10 days) Atlantic blocks are captured by the model better than long Pacific blocks, but for blocks of intermediate duration a mixed situation prevails.

These two figures provide some additional information about the ability of the model to exit blocks correctly. Much more attention has usually been devoted to the onset forecasting problem, i.e. the zonal-to-blocking transition, but less attention is usually paid to the corresponding problem of blocking-to-zonal transition. Figs. 15 and 16 show that often the model fails to exit a blocking condition at the correct time, persisting in a blocked state which is no longer observed. It is interesting to point out how this fact, together with the information contained in Figs. 5 and 6, affects the interpretation of the results shown in Fig. 1. The cumulative measure of model blocking frequency, computed irrespectively of correct verification of the forecast (as the curves of Fig. 1, panels e to l, effectively are), hides the fact that, by day ten, more than 50% of the events which contribute to the frequency do not verify correctly (see Figs 5 and 6). If, for example, Fig. 1i were redrawn using only correctly verified 3- or 5-day forecasts, the already low model peaks in correspondence of Atlantic and Pacific blocking would be further reduced, leaving little signal.

6. Blocking and forecast skill in the NH

Another very interesting way to study the impact of blocking on medium-range predictions is to stratify objective model skill according to the observed prevailing weather regime. This allows an objective, quantitative evaluation of common, but often unproven, beliefs which make blocking a favourable condition for numerical forecasting. Before going into a more detailed analysis of the results it is perhaps useful to recall the heuristic basis for the above mentioned belief.

Numerical models have, for the most part of their early history, been affected by the tendency (or, rather, systematic error) to show too much of a persistent dynamical behaviour and correspondingly too little high- and low-frequency variability. This generic behaviour, common to many, if not all, early numerical forecasting models, has produced the belief that persistent atmospheric regimes (of which blocking is an outstanding example) favour numerical weather prediction, in the sense that they go in the direction of minimizing the effects of model systematic error. If this simplistic argument were entirely correct, one would expect objective model performance measure to reflect this by showing measurable differences in ensemble means of model skillscores stratified according to the regime prevailing in the initial conditions (ICs). More precisely, one would expect forecasts starting from blocked ICs to be on average more skilful than forecasts starting from zonal ICs. A third group of forecasts, which would score last in this list, is the one formed by ten day forecasts during which a significant regime transition takes place. Given the unstable nature of the regime transition, and on the basis of the results diagnosed so far, it can be safely assumed that these forecasts should be the least successful.

To determine forecast skill, the choice of an objective measure is required. The one used here will be Anomaly Correlation Coefficient (ACC) of 500 hPa geopotential height computed over the relevant sectors of the Northern Hemisphere (Pacific or Euro-Atlantic). The limitations of this objective skillscore are well known, e.g. Palmer and Tibaldi, 1988; Murphy, 1991. This measure of skill was however preferred to the more usual RMS error because of its sensitivity to flow shape and structures, rather than to absolute geopotential height values, a characteristic which appears desirable during blocking situations. The climate used to compute anomalies is the corresponding entire seven years seasonal climate. To stratify forecasts according to the grosswetterlage prevailing during the forecast period, an objective criterion is also needed. Here the following was chosen, on the sole ground of reasonability and ease of implementation. Forecasts started on the day of blocking onset, 1 and 2 days later have been classified as the "blocking ensemble", forecasts started 4, 5, and 6 days before blocking onset have been classified as the "transition ensemble", and all the forecasts with no blocking events throughout the integration period have been classified as the "zonal ensemble".

Figures 17 and 18 summarize the results of this analysis. The only cases where the above-mentioned simple logic (best forecasts during blocking situations, next best during zonal conditions, worst when a zonal-to-blocking transition occurs) is completely borne out by model behaviour are Winter and Autumn Pacific blocking and Summer Euro-Atlantic blocking. A second type of model behaviour is observed

during Euro-Atlantic blocking in Spring and Winter and for Pacific blocking in Spring and Summer, i.e. best forecasts during zonal conditions, next best during blocking and worst of all during transitions. The Pacific sector during Summer behaves similarly, with zonal situations scoring better than both blocking and transitional regimes. The only period during which transition forecasts score best is Autumn in the Euro-Atlantic sector. In this last case, however, relative differences are very small. Additionally, Autumn is a season during which blocking in the Atlantic is relatively weak and rare. In general, the model has more difficulties if a transition occurs within forecasting range during those seasons when blocking activity is vigorous.

A conclusion emerging from the above results is that, while the zonal-to-blocking transition is a serious problem for numerical model forecasting during all seasons and in both NH sectors, at least as far as ACC is concerned, serious forecast failures are also common during both persistent blocking and persistent zonal situations. This attempt to diagnose a possible blocking-skill relationship does not provide any additional information as far as the origins of errors in the two different regimes. It is possible to speculate that smaller, more rapid, baroclinic scales could dominate error patterns during zonal regimes, while larger, slightly slower and more barotropic processes would dominate the generation of forecast errors during persistent blocking situations, including failures to correctly maintain the observed blocked structure. This problem is in need of further investigations, possibly based on more detailed case studies, and will be the subject of future work.

7. Blocking in the Southern Hemisphere

Before discussing the extension of the analysis to the Southern Hemisphere, a description of the modifications to the index definitions appropriate for the SH is needed. These affect the latitudes at which geopotential height gradients are evaluated. The need for such a change is explained by the fact that blocks in the Southern Hemisphere are usually located at lower latitudes than Northern Hemisphere blocks, see Taljaard (1972), Coughlan (1983), Lejenäs (1984), and Økland and Lejenäs (1987).

To define the index in the Southern Hemisphere, the geopotential height gradients GHGN and GHGS (respectively middle and high latitudes) are again evaluated at each longitude point of the grid as:

$$GHGS = [z(\phi_S) - z(\phi_0)]/(\phi_S - \phi_0) \quad (8.1)$$

$$GHGN = [z(\phi_0) - z(\phi_N)]/(\phi_0 - \phi_N) \quad (8.2)$$

where

$\phi_N = 35°S + \Delta$
$\phi_0 = 50°S + \Delta$
$\phi_S = 65°S + \Delta$

and $\Delta = -3.75°, 0°, +3.75°$

A given longitude is then defined to be blocked at a certain instant in time if the following conditions are both satisfied for at least one value of Δ:

$$GHGN > 0 \quad (8.3)$$

$$GHGS < -10.\ m/(^\circ \text{ latitude}) \quad (8.4)$$

Condition (8.4) was added (as for the NH case), to ensure that cut-off lows anomalously displaced to the South were not counted as blocks.

The result of the local and instantaneous index calculation on the analyses in our database is shown in the top panels of Fig. 19 (a to d). The season definition is of course specular with respect to the one used for the Northern Hemisphere: Winter indicates the JJA (June, July and August) period, Spring is SON, Summer is DJF and Autumn is MAM. As it has been the case for the Northern Hemisphere, for the Southern Hemisphere as well the TM modified version of the Lejenäs and Økland index behaves in a very similar way to the original index, as it can be seen from a comparison of Fig. 19 with Fig. 2 of Lejenäs (1984).

Compared to their Northern Hemisphere counterparts, Southern Hemisphere blocking events show a simpler picture. They are overall much less frequent, and do not show strong seasonal dependence. During Winter, there is only one area, very wide in longitude, of maximum frequency, extending from 150° E to 70° W. This broad area has two relative maxima. The first maximum, localized between 150° E and 210° E, has a frequency of occurrence above 10%, and remains above this level for the whole year, with very small seasonal variations of intensity. This sector can be identified with the Australia-New Zealand blocking region. The other maximum, from 70° W to 100° W, has a frequency of occurrence between 5% and 10%, is localized East of the South American coast, and can be identified as the Andes blocking area. With the march of the seasons, the blocking frequency in the Andes area decreases, and reaches its minimum value in Summer, when the signal is undistinguishable from the background noise. In Autumn there are signs of an increasing blocking activity and the frequency starts to rise again. It is worth noting here that, with the possible exclusion of the Winter period, when it has its maximum value, the frequency of blocking occurrence in the Andes area, as it appears from our index, is very low, and does not appear to give an important contribution to the global blocking activity of the Southern Hemisphere.

As in the case of the Northern Hemisphere, the geographical localization of blocking suggests an analysis that considers sectors instead of isolated longitudes. Following the same criteria used before, an Australian sector has been defined with the longitudinal limits 150° W; 150° E. The sector definition is kept fixed for all seasons.

The results of this sector blocking definition are summarized in Table 2, which contains the number of blocking days identified in the Australian sector, and in Figure 20, which shows the seasonal march of sector blocking days frequency. The further application of the condition on time duration (blocking cases defined as episodes longer than five days) gives the results contained in the second column of Table 2. From the table it is evident that about 30% of the days are blocked all over

the year (see Fig. 20), and, as previously noted, only a slight seasonal trend is detectable with a certain predominance of Winter, both in terms of blocking days and number of cases.

In parallel to what we did for the NH, we show here the signature of the Australian blocked regime in Fig. 21. The differences between the observed fields at 500 hPa in the ensembles of "blocked" and "zonal" days are shown for the different seasons (Winter to Autumn, panels a to d respectively). As it was the case for NH blocking signatures, the shape of the patterns appear synoptically realistic, which justifies aposteriori the choices made to define the objective index. As already noted, SH blocking shows less of a seasonal cycle and slightly weaker features (at least for those seasons, like winter, which have the strongest blocking in the NH).

7.1 Short- and medium-range forecast of blocking in the SH

The results of the application of the local and instantaneous index to the predicted fields (day 3 and day 10 forecasts, as for the Northern Hemisphere) are shown in the middle (e to h) and bottom (i to l) panels of Figure 19 respectively, the dotted line in all panels refers to the observations, and has been superimposed to facilitate the comparison. A general trend, detectable in all seasons (and already noted for the NH), is the decrease of the blocking frequency with the increase of the forecast period. Already at day 3 the blocking frequency starts to decrease and, particularly in Winter and Spring, its maximum shifts to the East. At day 10 the simulated blocking frequency becomes so low to be almost undistinguishable from the background noise. The number of correctly predicted blocked days versus forecast time is shown in Fig. 22 and does not differ substantially for the corresponding figures (5 and 6) presented for the Northern Hemisphere. Also in the case of the Australian blocking there is an almost exponential decrease in the number of correct forecasts.

The systematic errors in the strength and position of the correctly predicted blocking-like structures are presented in Fig. 23 and Fig. 24 respectively. The mean error (mean over the correctly forecasted days) in the blocking index indicates a general underestimation of the amplitude of the blocks. The forecast of the position of the block has a clear eastward shift only during Winter. For all the other seasons the tendency towards an eastward shift is characteristic only of the first forecast days. A feature common to both the amplitude and the position of the forecasted blocks is a return of forecast skill after forecast day 7. This return of skill has been observed also in the Northern Hemisphere blocking and there is no simple and unambiguous explanation for it. A possible explanation could be that only very persistent, and therefore predictable blocks, can be forecasted seven or more days in advance, and so the statistics of these forecast times is representative only of the long lasting episodes. At this stage, however, this remains only a speculation.

7.2 Blocking onset and blocking duration in the SH

The performance of the ECMWF model in forecasting blocking onset is shown in Fig. 25, which summarizes the results obtained for the Australian sector. The prediction of blocking onset in the Southern Hemisphere as an initial value problem appears to be a difficult task for the ECMWF model, even at very short range. This appears to be the most evident difference between the model's behaviour in the two hemispheres. Neglecting, for the moment, medium range forecasts, for which correct forecasts are almost completely absent, in the short range, 1-3 days, the success rate is much lower than that found for Northern Hemisphere blocking. In fact the success rate for day 1 forecast is only 70% (50 successes over 71 cases), and drops to 42% (30/71) for day 2 forecast. The corresponding rates for the Northern Hemisphere Atlantic blocking are 88% (77/88) for day 1 and 60% (53/88) for day 2, and, for Pacific blocking, 80% (51/64) for day 1 and 63% (40/64) for day two). There is no appreciable seasonal cycle in the behaviour of the model.

Although it is always difficult to put forward essentially unsubstantiated interpretations, the most likely reason for the different performance of the model in the two hemispheres could be found in the different availability of observations, which strongly influences the accuracy of the initial conditions, so that better analyses in the Northern Hemisphere lead, on average, to a better operational predictability of blocking events.

The performance of the ECMWF model in predicting the duration of Southern Hemisphere blocking is shown in Fig. 26; it is evident that in general the model underestimates the duration of the blocking episodes. In 66% of the cases the predicted block is shorter than observed; in 24 % of the cases the predicted duration is correct, while predicted blocks last longer than observed only in the remaining 10% of the cases. More information about the behaviour of the model in predicting the duration of the blocking episodes can be derived from the inspection of Fig. 27, where the histograms of the number of episodes as a function of duration are shown. Moving towards longer block durations, it is possible to note a decrease in the number of predicted cases which is higher than the observed decrease.

7.3 Forecast skill and blocking in the SH

Observed differences between blocking in the two hemispheres are usually ascribed to geographical differences (e.g. mountains and land-sea contrasts) and to dynamical differences (e.g. the different role played by ultra-long planetary waves). The results presented and discussed above point out towards an additional important difference between the behaviour of the ECMWF model in the two hemispheres, which reflects an increased difficulty (compared to the situation in the NH) to forecast, even at short range, blocking onset in the Southern Hemisphere.

A possible explanation, as suggested above, to justify this lower SH predictability of blocking onset has been the lower accuracy of the atmospheric analysis used as initial condition. This lower accuracy, in turn, is most likely due to lack of observations. If

this interpretation is correct, we should expect, in the Southern Hemisphere, a lower forecast skill than in the Northern Hemisphere not only for blocking onset, but for all other weather regimes as well.

The objective forecast skill in the two hemispheres can be evaluated comparing the ACC composited according to different weather regimes shown in Figs. 17 and 18, referring to NH Euro-Atlantic and Pacific Blocking respectively, with Fig. 28, referring to SH Australian blocking. The differences between the two hemispheres stand out clearly. In the Northern Hemisphere, appreciable differences during "blocked", "zonal", and "transition" regimes are evident, while in the Southern Hemisphere the behaviour of the model does not show any significant systematic difference between the various regimes. The comparison also confirms the generally lower forecast skill in the Southern Hemisphere compared with the Northern Hemisphere, both for the short- and medium-range. The rate of decrease of the ACC typical of the day 2-day 6 period of the SH is attained, in the NH, seldom and only *after* day 6. Such results are consistent with two alternative interpretations: either this regime classification is unable, in the SH, to show any measurable predictability difference between the regimes, or the predictive capabilities of the forecasting system in the SH (observational network, data assimilation system and forecasting model) are insufficient to show the subtle differences in predictability among the weather regimes.

8. Summary and conclusions

The analysis performed on seven years of ECMWF operational Lorenz files, i.e. 500 hPa geopotential height data, both analyzed and predicted, has revealed a significant seasonal variability of the frequency of blocking episodes in both the Euro-Atlantic and Pacific sectors of the Northern Hemisphere, as they are detected by an objectively defined synoptic-type index. Such index (a modification of the original Lejenäs and Økland index) allows a separate analysis of blocking predictability in the two preferred Northern Hemispheric sectors, i.e. Euro-Atlantic and Pacific. The Winter-Spring extended season emerges as the most active period for Atlantic blocking, whereas blocking in the Pacific sector is more probable during the more extreme seasons of Winter and, to a lesser degree, Summer.

For the Northern Hemisphere, the model performance also shows some considerable seasonal dependence, with the best predictive results obtained for the Atlantic and Pacific sector blocking during Spring. However, the model exhibits difficulties in representing blocking with the correct frequency and amplitude that are rather uniformly distributed through the year. In particular, there is a general tendency to underestimate blocking intensity, with the notable exception of Autumn in the Euro-Atlantic sector. Spring appears to be the period of the year during which blocking intensity is best predicted, in both sectors of the Northern Hemisphere. The model performance is in general slightly better over the Atlantic sector than it is over the Pacific, indicating that the physical mechanisms responsible for Atlantic and Pacific blocking might be at least partially different.

Large phase (longitude) errors of opposite sign and increasing with forecast time are evident in modelling the evolution of blocking, corresponding to a model eastward shift of Atlantic blocks and to a model westward shift of Pacific blocks. Such phase errors, however, almost vanish during transition seasons (Spring and Autumn) to become very large in Winter and Summer, in agreement with Tibaldi and Molteni's (1990) results. The above conclusions on the adequacy of the model's blocking climatology are drawn without distinguishing, for a given forecast day, between verified and unverified blocking occurrencies. It is quite possible that such results could be modified by removing unverified (wrongly forecasted) blocks from the data set. This, however, would impoverish too much the data base, and even more so for late forecast days.

Predicting blocking onset is confirmed to be a difficult task for the model, with no clear seasonal cycle or long term trend, at least in the seven year period analyzed here, but see the results of Tibaldi et al (1993) on more recent Winter data. The performance of the model on blocking maintenance, on the contrary, is on average good, with a number of outstanding successes in predicting long-lasting blocks, and almost as many overpredictions of blocking duration as underpredictions.

Regarding blocking and objective skillscores, the commonly expected situation of "best forecasts during blocking situations, next best during zonal conditions, worst when a zonal-to-blocking transition occurs" is actually verified only in Winter and Autumn Pacific blocking and Summer Euro-Atlantic blocking. A second, common case is that forecasts during zonal and blocked situations are equally easy (or equally difficult) to make, while zonal-to-blocking transitions are by far the most difficult situations to predict (the case for the Euro-Atlantic sector in Spring and Winter and for the Pacific sector in Spring and Summer).

The shape and intensity of the synoptic structures typical of blocking (the blocking signatures) have been shown to possess an evident seasonal cycle in both sectors of the NH; this seasonal cycle is much weaker in the SH. Model systematic errors (SEs) are described by horizontal spatial structures which are similar, but with the opposite sign, to those typical of the blocking signature. This is confirmed to be more evident during the NH Winter season. During the other seasons, SEs appear to be weaker in intensity.

We have also assessed the skill of the model in short and medium range forecast of blocking in the Southern Hemisphere. The comparison of results obtained for the Northern Hemisphere shows that the behaviour of the model is very similar in the two hemispheres with only one important difference: the skill in the prediction of the blocking onset, even for short range forecast, is much lower in the Southern Hemisphere than it is in the Northern Hemisphere. The lower accuracy of the initial analyses (due to the comparative lack of observations in the Southern Hemisphere) can partially account for this result. This idea is strengthened by fact that the overall forecast skill in the Southern Hemisphere is confirmed to be lower than in the other hemisphere.

Acknowledgements

This work has been partially supported by CNR of Italy, Progetto Finalizzato "Sistemi Informatici e Calcolo Parallelo" and by CEC, EPOCH Programme (C21C Project). The contributions of F. Molteni and R. Mureau of ECMWF in terms of providing data, assistance and useful exchanges of ideas are gratefully acknowledged. F. D'Andrea provided useful comments on an early version of the manuscript.

References

Arpe K., 1990: Impacts of Changes in the ECMWF Analysis-Forecasting Scheme on the Systematic Error of the Model. Proceedings of the ECMWF 1989 Seminars on "Ten Years of Medium Range Weather Forecasting", Reading, 4-8 September, 1989. Available From ECMWF, Reading, Berks., UK.

Brankovic C. and L. Ferranti, 1992: Seasonal integrations with realistic boundary forcing. ECMWF Workshop on "New developments in predictability", 305-333.

Coughland M.J., 1983: A Comparative Climatology of Blocking Action in the Two Hemispheres. Austr. Met. Mag., **31**, 3-13.

Dole, R.M. and Gordon N.D., 1983: Persistent anomalies of the extratropical Northern Hemisphere wintertime circulation: geographical distribution and regional persistence characteristics. Mon. Wea. Rev., **111**, 1567-1586.

Grønaas S., 1983: Systematic error and forecast quality of ECMWF forecasts in different large-scale flow patterns. ECMWF Seminar/workshop on Interpretation of NWP products, 13-24 September 1982, 161-206. ECMWF, Shinfield Park, Reading, UK.

Lau, L.-C., 1983: Mid-latitude wintertime circulation anomalies appearing in a 15-year GCM experiment. In: Large scale dynamical processes in the atmosphere (eds. B.J. Hoskins and R.P. Pearce) New York: Academic Press, 111-125.

Lejenäs H., 1984: Characteristics of Southern Hemisphere Blocking as Determined from a Time Series of Observational Data. Quart. J.R. Met. Soc., **110**, 967-979.

Lejenäs H. and H. Økland, 1983: Characteristics of Northern Hemisphere Blocking as Determined from a Long Time Series of Observational Data. Tellus, **35A**, 350-362

Miyakoda K. and J. Sirutis, 1990: Sub-grid Scale Physics in 1-Month Forecasts. Part II: Systematic Error and Blocking Forecasts. J. Atmos. Sci., **118**, 1065-1081.

Murphy A.H., 1991: Forecasts verification: its complexity and dimensionality. Mon. Wea. Rev., **119**, 1590-1601.

Økland H. and H. Lejenäs, 1987: Blocking and Persistence. Tellus, **39A**, 33-38.

Palmer, T.N. and S. Tibaldi, 1988: On the prediction of forecast skill. Mon. Wea. Rev., **116**, 2453-2480.

Ruti P., 1992: La rappresentazione delle situazioni di blocco nei modelli di circolazione generale dell'atmosfera. Doctor Thesis, Available from University of Bologna, Dept. of Physics, Via Irnerio 46, 40126 Bologna, Italy.

Taljaard J.J., 1972: Synoptic Meteorology of the Southern Hemisphere. in Meteorology of the Southern Hemisphere, C.N. Newton (Editor), Meteor. Monogr., **13**, 139-211.

Tibaldi, S., 1993: Low-Frequency Variability and Blocking as Diagnostic Tools for Global Climate Models. Proceedings of the NATO Advanced Research Workshop on "Prediction of Interannual Climate Variations". Ed. J. Shukla. NATO-ASI Series, Springer-Verlag, 173-182.

Tibaldi S. and F. Molteni, 1990 (TM): On the Operational Predictability of Blocking. Tellus, **42A**, 343-365.

Tibaldi S., T.N. Palmer, C. Brankovic and U. Cubasch, 1991: Extended-Range Predictions with ECMWF Models: Influence of Horizontal Resolution on Systematic Error and Forecast Skill. Q.J.R. Meteorol. Soc., **116**, 835-866.

Tibaldi S., P. Ruti, E. Tosi and M. Maruca, 1993: Operational predictability of Winter Blocking: an ECMWF update. Proceedings of the ECMWF Seminars on "Validation of forecasts and large-scale simulations over Europe", Reading, 7-11 September 1992. Available from ECMWF, Reading, UK.

Tracton M.S., 1990: Predictability and its relationship to scale interaction processes in blocking. Mon. Wea. Rev., **118**, 1666-1695.

Tracton M.S., K. Mo, W. Chen, E. Kalnay, R. Klister and G. White, 1989: Dynamical extended range forecasting (DERF) at the National Meteorological Centre. Mon. Wea. Rev., **117**, 1604-1635.

Season	Blocking days		Blocking cases	
	E.A.	PAC.	E.A.	PAC.
Winter	281	285	27	25
Spring	357	182	29	11
Summer	194	204	14	20
Autumn	209	99	18	8

Table 1 This table shows the total number of blocking days (which satisfy the criterion of three adjacent longitudes blocked in a sector), and blocking cases (which satisfy also the requirement on the minimum duration of five days) for the Euro-Atlantic and Pacific sectors

Season	Blocking days	Blocking cases
Winter	249	21
Spring	190	15
Summer	184	17
Autumn	222	18

Table 2 As for Table 1, but for the Australian sector of the Southern Hemisphere.

Figure captions

Figure 1 - Percentage frequency of blocked days in the Northern Hemisphere as a function of longitude computed for each day in the analyses (first row), day 3 forecasts (second row) and day 10 (third row); first column Winter (DJF), second column Spring (MAM), third column Summer (JJA), and fourth column Autumn (SON).

Figure 2 - Percentage of blocked days for each decade of the year. a): Euro-Atlantic blocking; b): Pacific blocking.

Figure 3 - Signatures of the regimes, i.e. differences between mean observed fields of 500 hPa height in the ensembles of "blocked" and "zonal" days, for the Euro-Atlantic sector (panels on the left, a to d) and for the Pacific sector (panels on the right, e to h). From top to bottom, Winter, Spring, Summer and Autumn. The isolines greater or equal to zero are continuous, negative isolines are dashed, the distance between isolines is 30 meters.

Figure 4 - Model day 10 500 hPa geopotential height total systematic errors (SEs, model ensemble mean minus observed ensemble mean) computed separately for each seasons. a) Winter, b) Spring, c) Summer and d) Autumn respectively. The isolines greater or equal to zero are continuous, negative isolines are dashed, the distance between isolines is 30 meters.

Figure 5 - Total and correct (shaded) forecasts of blocking in the Euro-Atlantic sector. a): Winter; b): Spring; c): Summer; d): Autumn.

Figure 6 - As in Fig. 3, but for the Pacific sector.

Figure 7 - Mean error in blocking intensity in the Northern Hemisphere. a): Winter; b): Spring; c): Summer; d): Autumn.

Figure 8 - Mean error in blocking phase (longitude) in the Northern Hemisphere. a): Winter; b): Spring; c): Summer; d): Autumn.

Figure 9 - Success/failure of forecast of blocking onset in the Euro-Atlantic sector. a): Winter; b): Spring; c): Summer; d): Autumn. A black square represents a correct forecast and a white square represents a failed forecast at a given forecast time. Forecast time along the ordinate and different blocking cases along the abscissa, grouped by different years. See also the text for more details.

Figure 10 - As in fig. 7, but for the Pacific sector.

Figure 11 - Number of correctly predicted onsets of blocking in the Euro-Atlantic sector as a function of increasing forecast time. a): Winter; b): Spring; c): Summer; d): Autumn.

Figure 12 - As in fig. 9, but for the Pacific sector.

Figure 13 - Forecast of blocking duration in the Euro-Atlantic sector. Black bars represent blocking duration in the analysis, and white bars represent blocking duration in the forecast. Black topped bars mean forecasted blocks shorter than observed and white topped bars mean forecasted blocks longer than observed. Totally black bars mean that the block duration has been correctly predicted. a): Winter; b): Spring; c): Summer; d): Autumn.

Figure 14 - As in fig. 9, but for the Pacific sector.

Figure 15 - Distribution of blocking duration in the Euro-Atlantic sector. a): Winter; b): Spring; c): Summer; d): Autumn.

Figure 16 - As in fig. 13, but for the Pacific sector.

Figure 17 - Anomaly Correlation Coefficient (ACC) of 500 hPa height between analysis and forecast as a function of forecast day in the Euro-Atlantic sector, computed on three different ensembles of cases, depending on the prevailing mean circulation: zonal (continuous line), blocked (short dashed line), and transition (dotted line). a): Winter; b): Spring; c): Summer; d): Autumn.

Figure 18 - As in fig. 15, but for the Pacific sector.

Figure 19 - Percentage frequency of blocked days in the Southern Hemisphere as a function of longitude computed for each day in the analyses (first row), day 3 forecasts (second row) and day 10 (third row); first column Winter (JJA), second column Spring (SON), third column Summer (DJF), and fourth column Autumn (MAM).

Figure 20 - Yearly cycle of the percentage of blocking days (for each decade) for Australian sector blocking.

Figure 21 - Signatures of observed blocking regimes for the Australian sector of the Southern Hemisphere, i.e. differences between mean observed fields of 500 hPa geopotential height in the ensembles of "blocked" and "zonal" cases referring to the Australian sector. Panels a to d, Winter, Spring, Summer and Autumn respectively. The isolines greater or equal to zero are continuous, isolines lesser than zero are dashed, the distance between isolines is 30 meters.

Figure 22 - Total and correct (shaded) forecasts of blocking in the Australian sector. a): Winter; b): Spring; c): Summer; d): Autumn.

Figure 23 - Mean error in blocking intensity in the Southern Hemisphere. a): Winter; b): Spring; c): Summer; d): Autumn.

Figure 24 - Mean error in blocking phase (longitude) in the Australian sector of the Southern Hemisphere. a): Winter; b): Spring; c): Summer; d): Autumn.

Figure 25 - Success/failure of forecast of blocking onset in the SH Australian sector. a): Winter; b): Spring; c): Summer; d): Autumn. A black square represents a correct forecast and a white square represents a failed forecast at a given forecast time. Forecast time along the ordinate and different blocking cases along the abscissa, grouped by different years. See also the text for more details.

Figure 26 - Forecast of blocking duration in the Australian sector. Black bars represent blocking duration in the analysis, and white bars represent blocking duration in the forecast. Black topped bars mean forecasted blocks shorter than observed and white topped bars mean forecasted blocks longer than observed. Totally black bars mean that the block duration has been correctly predicted. a): Winter; b): Spring; c): Summer; d): Autumn.

Figure 27 - Distribution of blocking duration in the Australian sector. a): Winter; b): Spring; c): Summer; d): Autumn.

Figure 28 - ACC between analysis and forecast as a function of forecast day. The ACC is computed only for the Australian sector, separately for the three categories of mean circulation: zonal (continuous line), blocked (short dashed line), and transition (dotted line). a): Winter; b): Spring; c): Summer; d): Autumn.

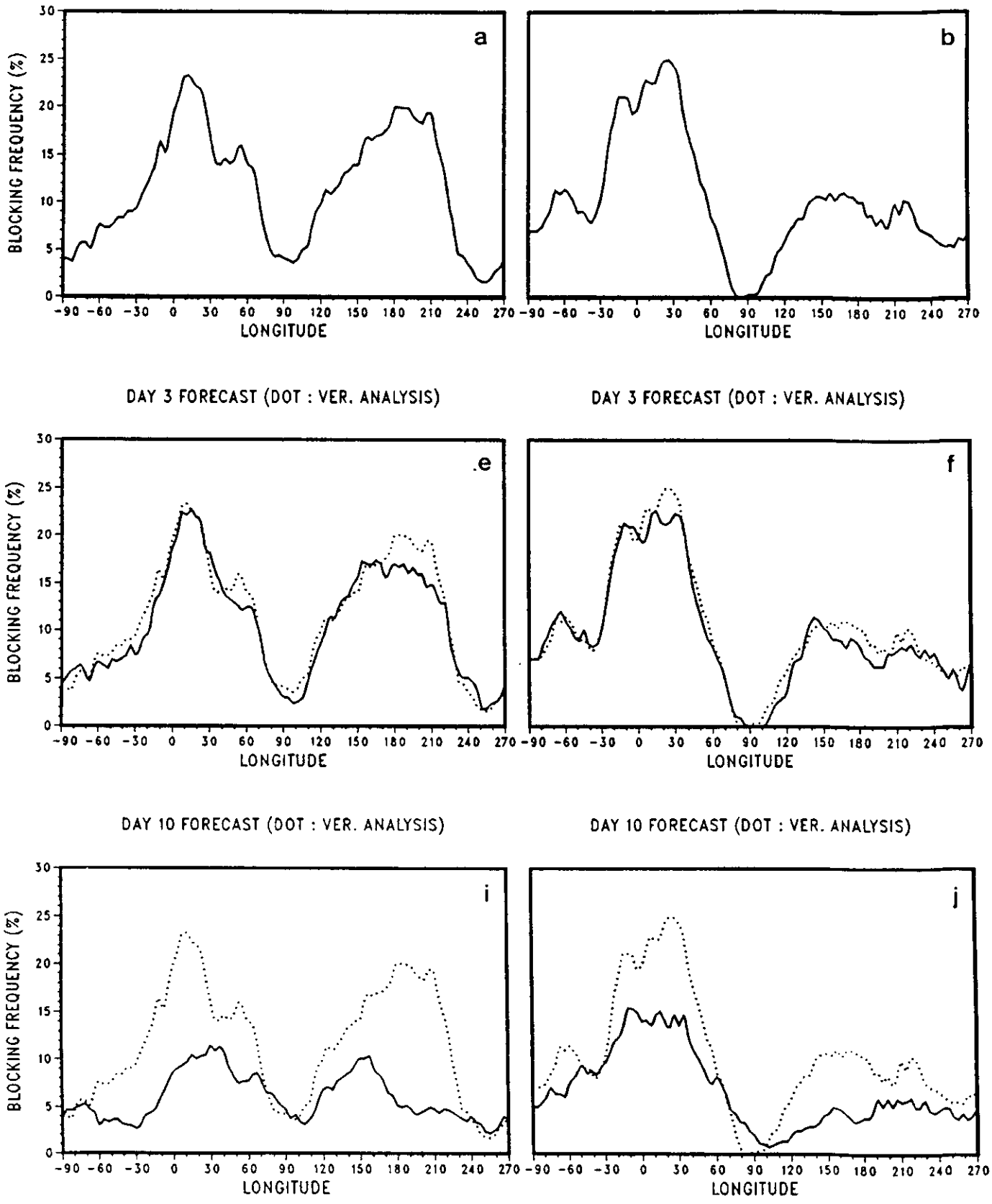
NH ANALYSIS (DEC–FEB 1981 to 1987)
NH ANALYSIS (MAR–MAY 1981 to 1987)
a
b
BLOCKING FREQUENCY (%)
LONGITUDE
DAY 3 FORECAST (DOT : VER. ANALYSIS)
DAY 3 FORECAST (DOT : VER. ANALYSIS)
e
f
DAY 10 FORECAST (DOT : VER. ANALYSIS)
DAY 10 FORECAST (DOT : VER. ANALYSIS)
i
j
-90 -60 -30 0 30 60 90 120 150 180 210 240 270
0 5 10 15 20 25 30

Fig 1 I

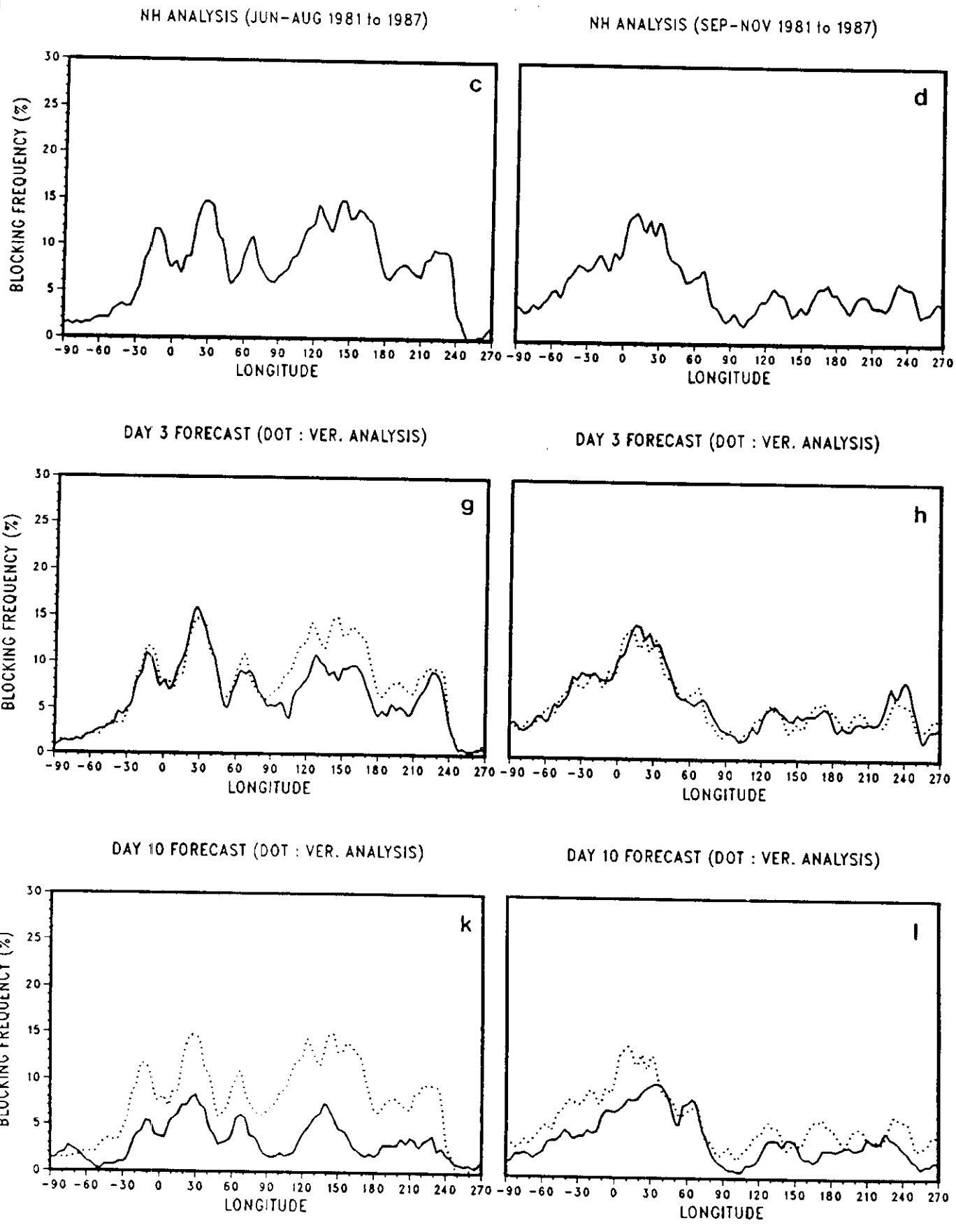
NH ANALYSIS (JUN–AUG 1981 to 1987)
NH ANALYSIS (SEP–NOV 1981 to 1987)
c
d
BLOCKING FREQUENCY (%)
LONGITUDE
DAY 3 FORECAST (DOT : VER. ANALYSIS)
DAY 3 FORECAST (DOT : VER. ANALYSIS)
g
h
DAY 10 FORECAST (DOT : VER. ANALYSIS)
DAY 10 FORECAST (DOT : VER. ANALYSIS)
k
l
-90 -60 -30 0 30 60 90 120 150 180 210 240 270
0 5 10 15 20 25 30

Fig 1 cont.

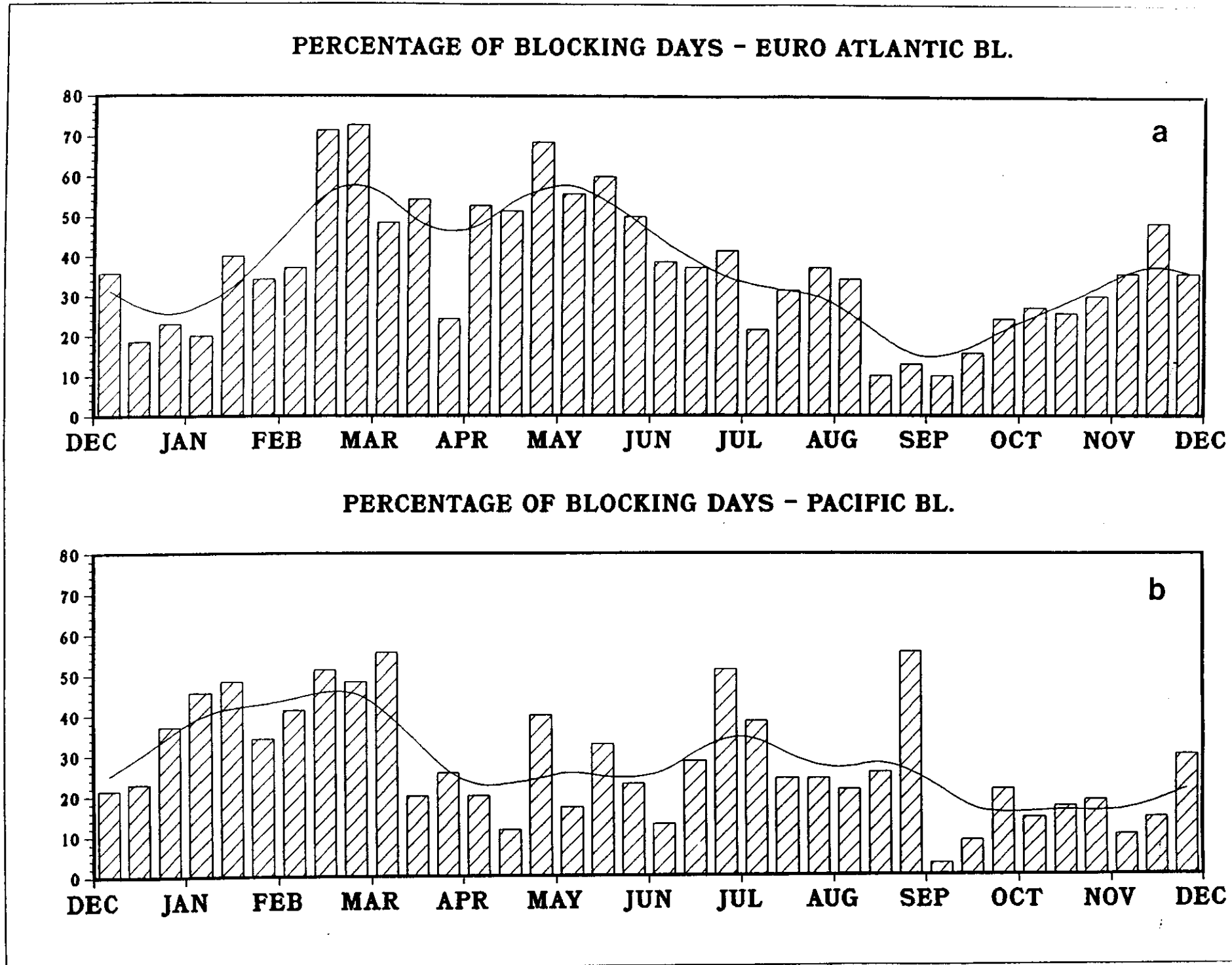
PERCENTAGE OF BLOCKING DAYS - EURO ATLANTIC BL.
a
80
70
60
50
40
30
20
10
0
DEC
JAN
FEB
MAR
APR
MAY
JUN
JUL
AUG
SEP
OCT
NOV
DEC
PERCENTAGE OF BLOCKING DAYS - PACIFIC BL.
b
80
70
60
50
40
30
20
10
0
DEC
JAN
FEB
MAR
APR
MAY
JUN
JUL
AUG
SEP
OCT
NOV
DEC

Fig 2

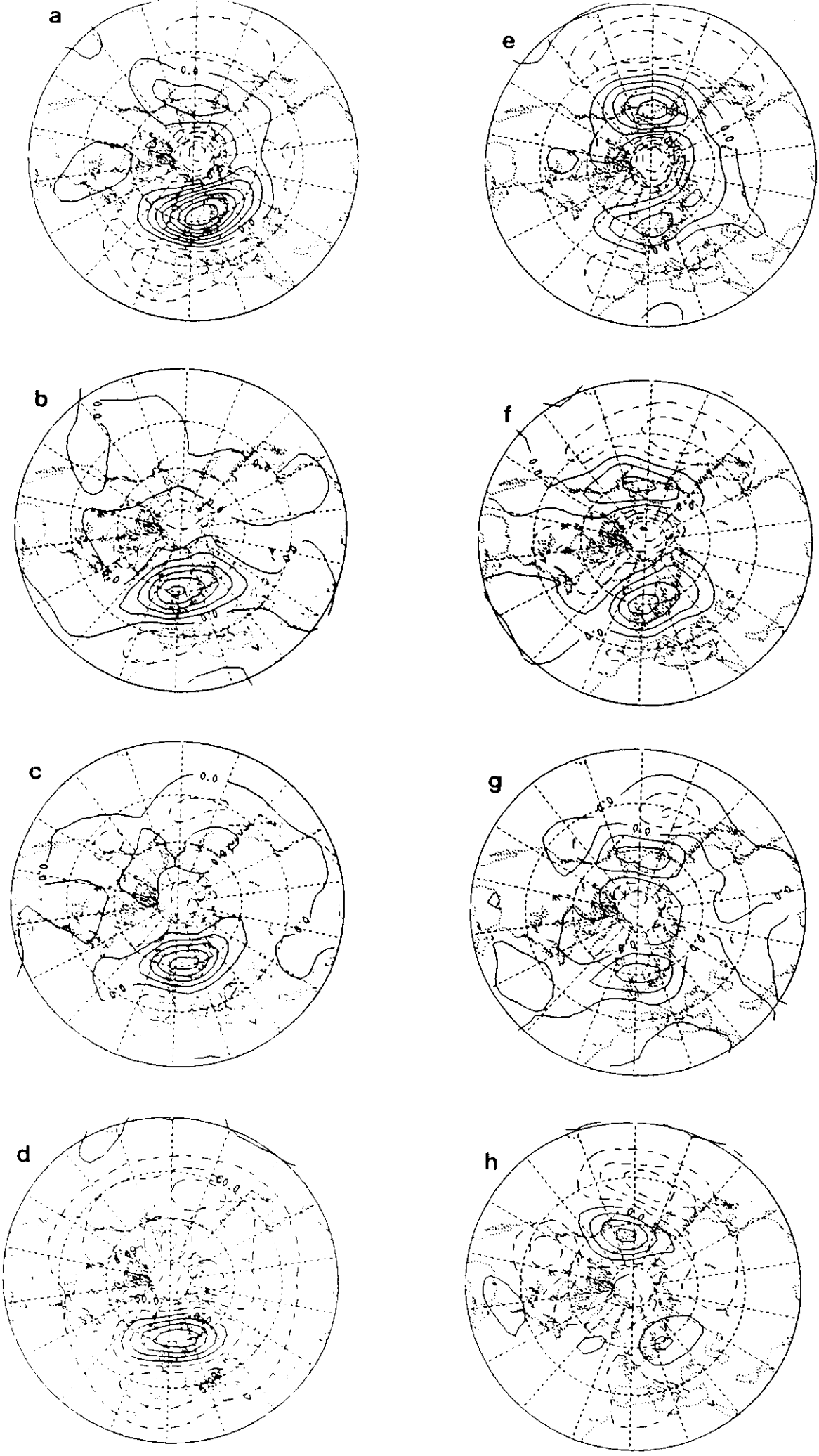

Fig 3

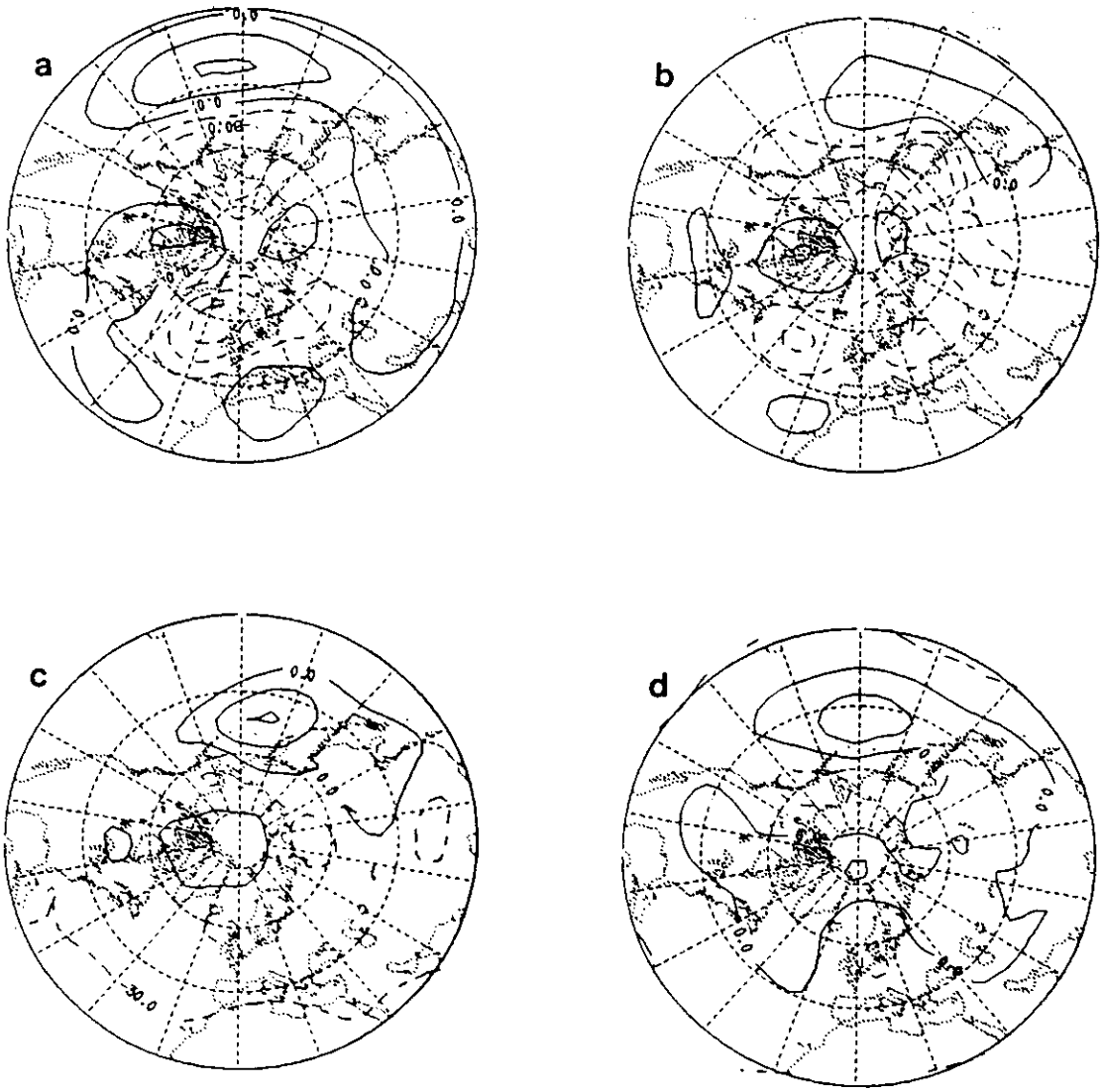

Fig 4

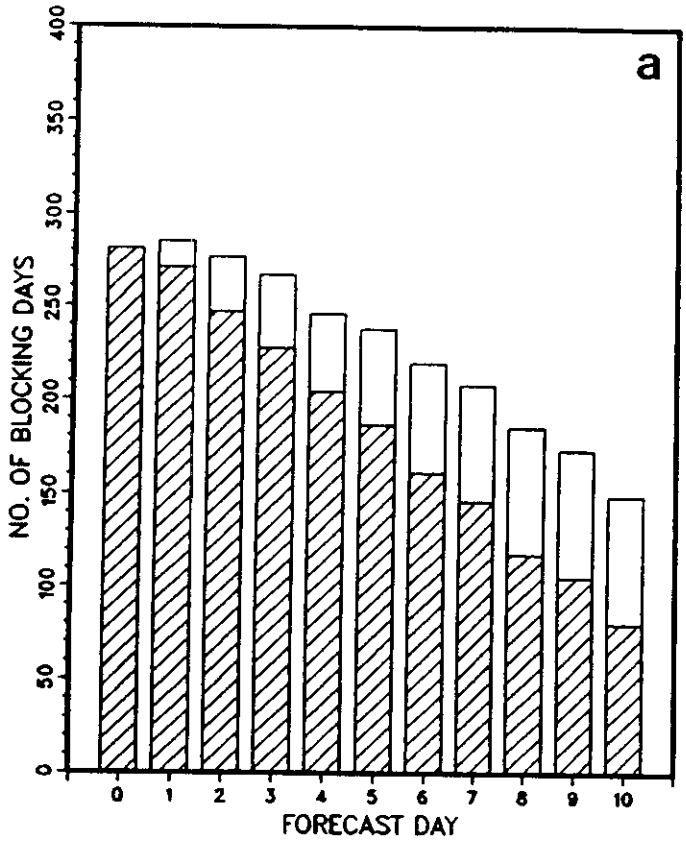
a
NO. OF BLOCKING DAYS
0
50
100
150
200
250
300
350
400
0 1 2 3 4 5 6 7 8 9 10
FORECAST DAY

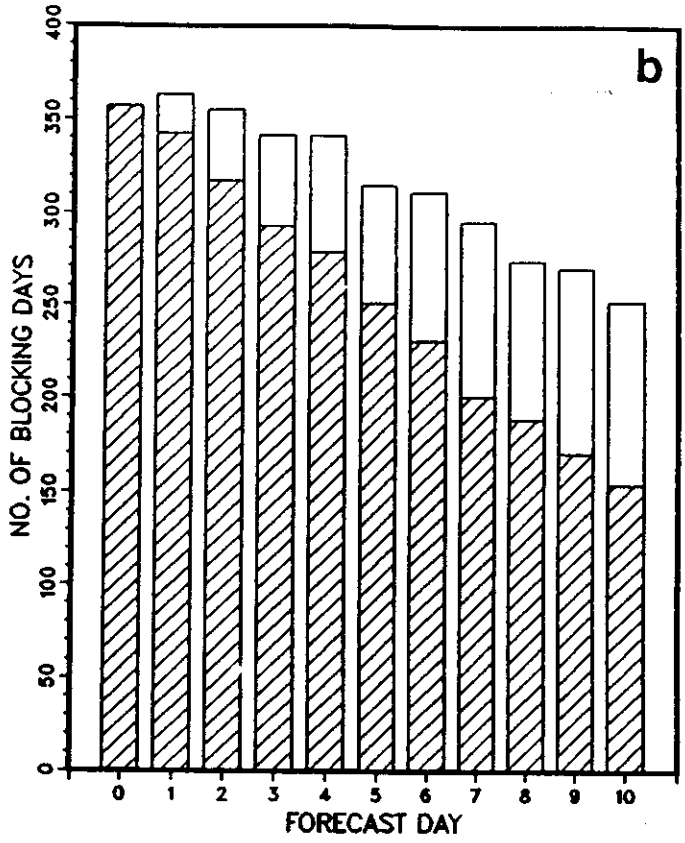
b
NO. OF BLOCKING DAYS
0
50
100
150
200
250
300
350
400
0 1 2 3 4 5 6 7 8 9 10
FORECAST DAY

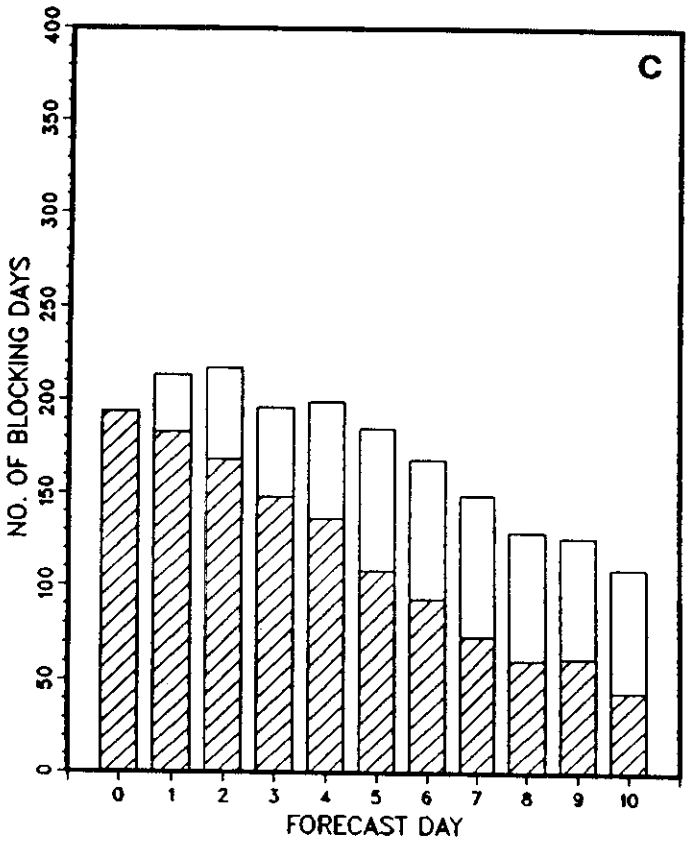
c
NO. OF BLOCKING DAYS
0
50
100
150
200
250
300
350
400
0 1 2 3 4 5 6 7 8 9 10
FORECAST DAY

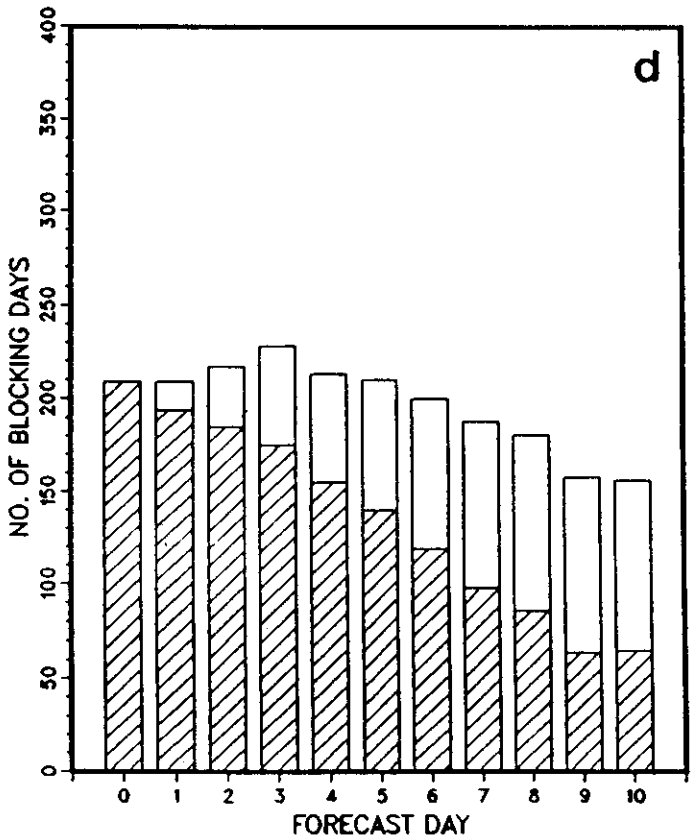
d
NO. OF BLOCKING DAYS
0
50
100
150
200
250
300
350
400
0 1 2 3 4 5 6 7 8 9 10
FORECAST DAY

Fig 5

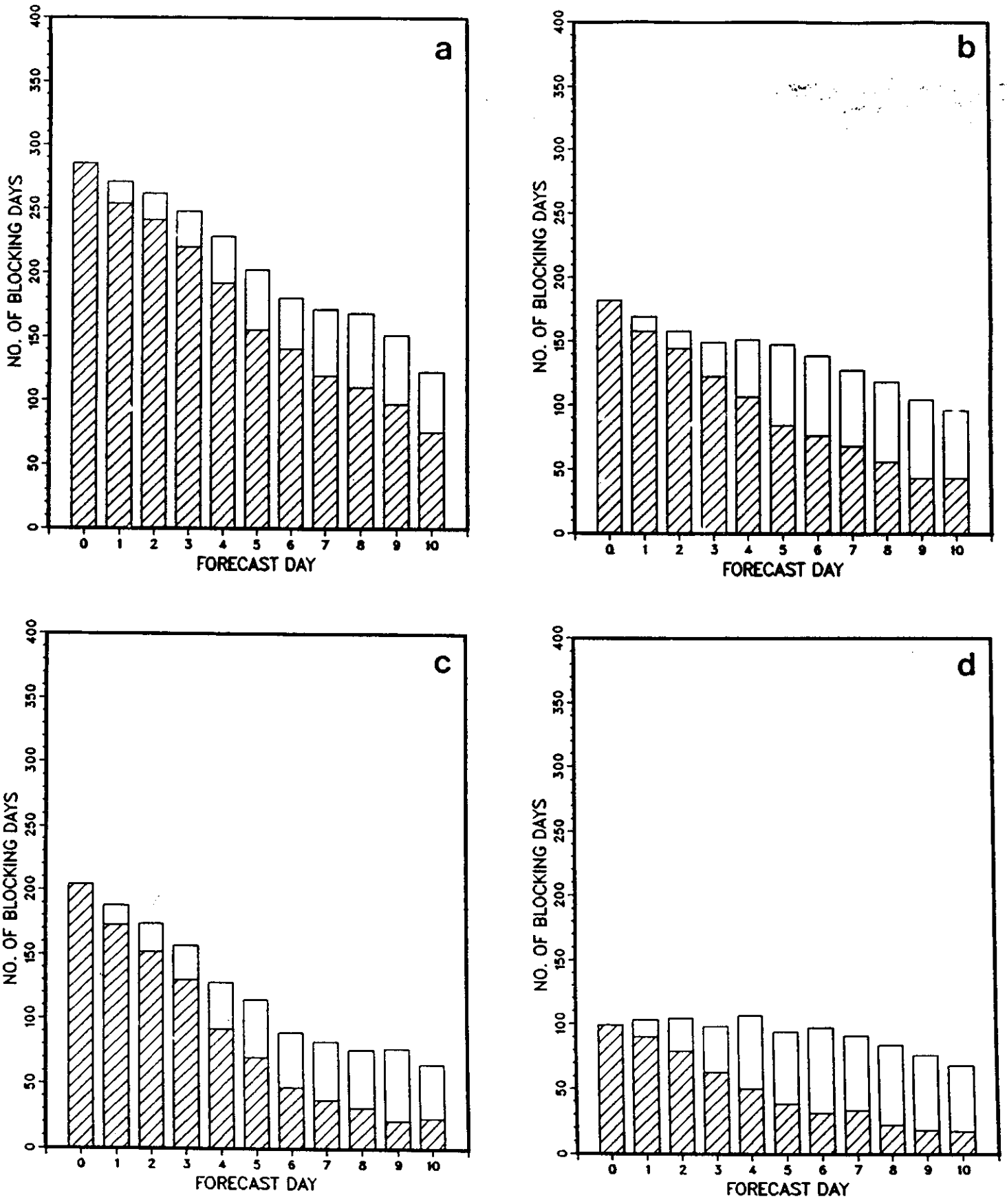
a
b
c
d
NO. OF BLOCKING DAYS
FORECAST DAY
0
50
100
150
200
250
300
350
400
0 1 2 3 4 5 6 7 8 9 10

Fig 6

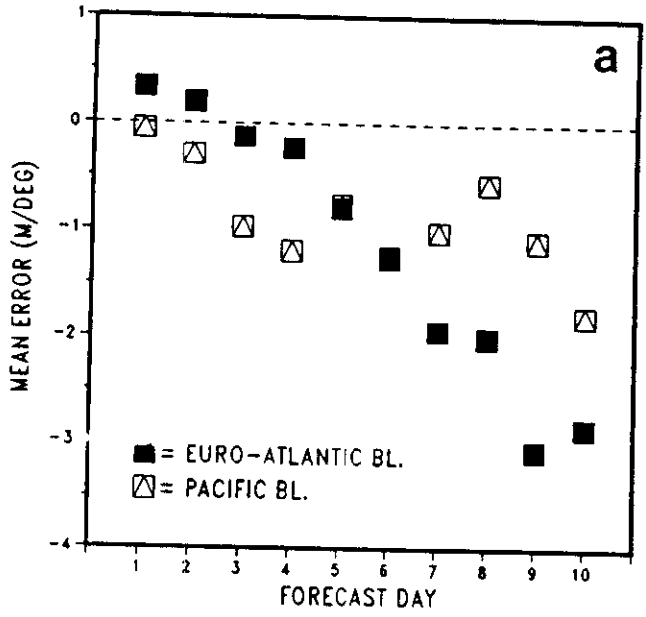
a
MEAN ERROR (M/DEG)
1
0
-1
-2
-3
-4
1 2 3 4 5 6 7 8 9 10
FORECAST DAY
= EURO-ATLANTIC BL.
= PACIFIC BL.

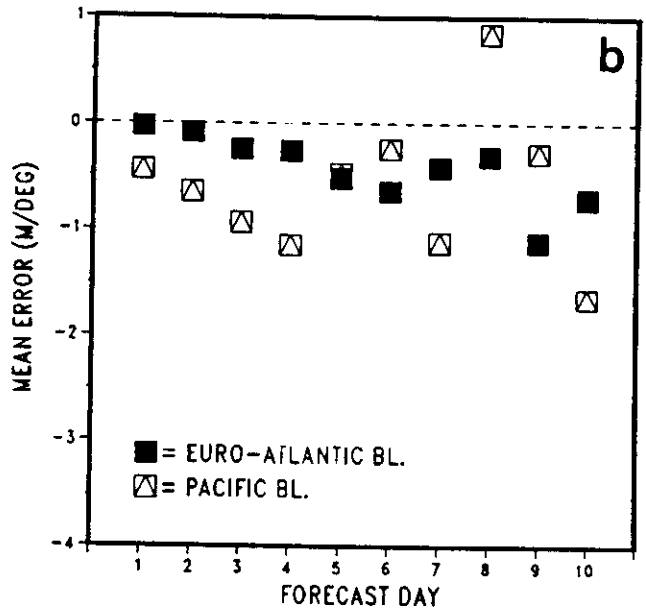
b
MEAN ERROR (M/DEG)
1
0
-1
-2
-3
-4
1 2 3 4 5 6 7 8 9 10
FORECAST DAY
= EURO-ATLANTIC BL.
= PACIFIC BL.

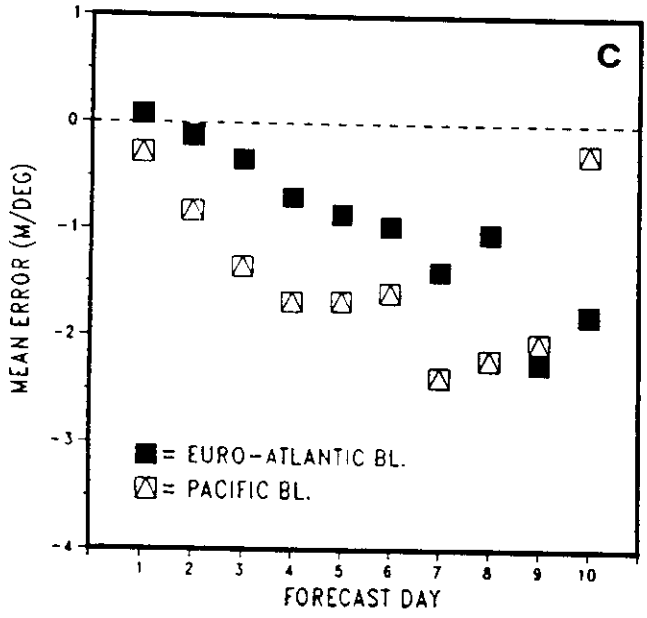
c
MEAN ERROR (M/DEG)
1
0
-1
-2
-3
-4
1 2 3 4 5 6 7 8 9 10
FORECAST DAY
= EURO-ATLANTIC BL.
= PACIFIC BL.

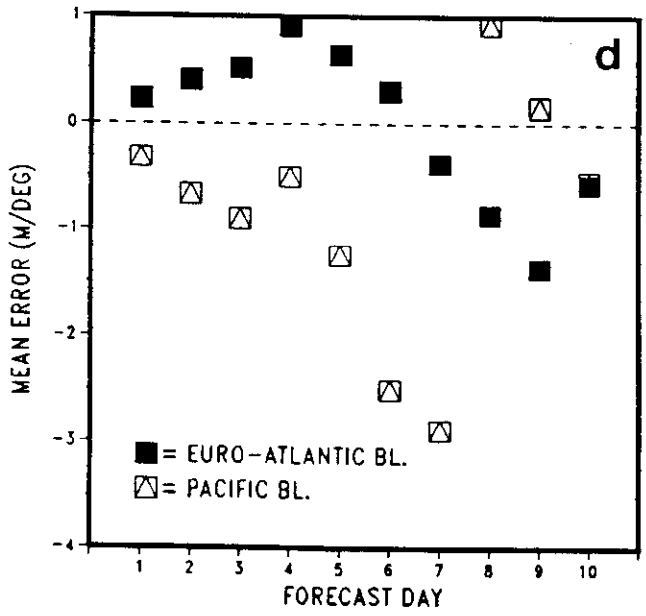
d
MEAN ERROR (M/DEG)
1
0
-1
-2
-3
-4
1 2 3 4 5 6 7 8 9 10
FORECAST DAY
= EURO-ATLANTIC BL.
= PACIFIC BL.

Fig 7

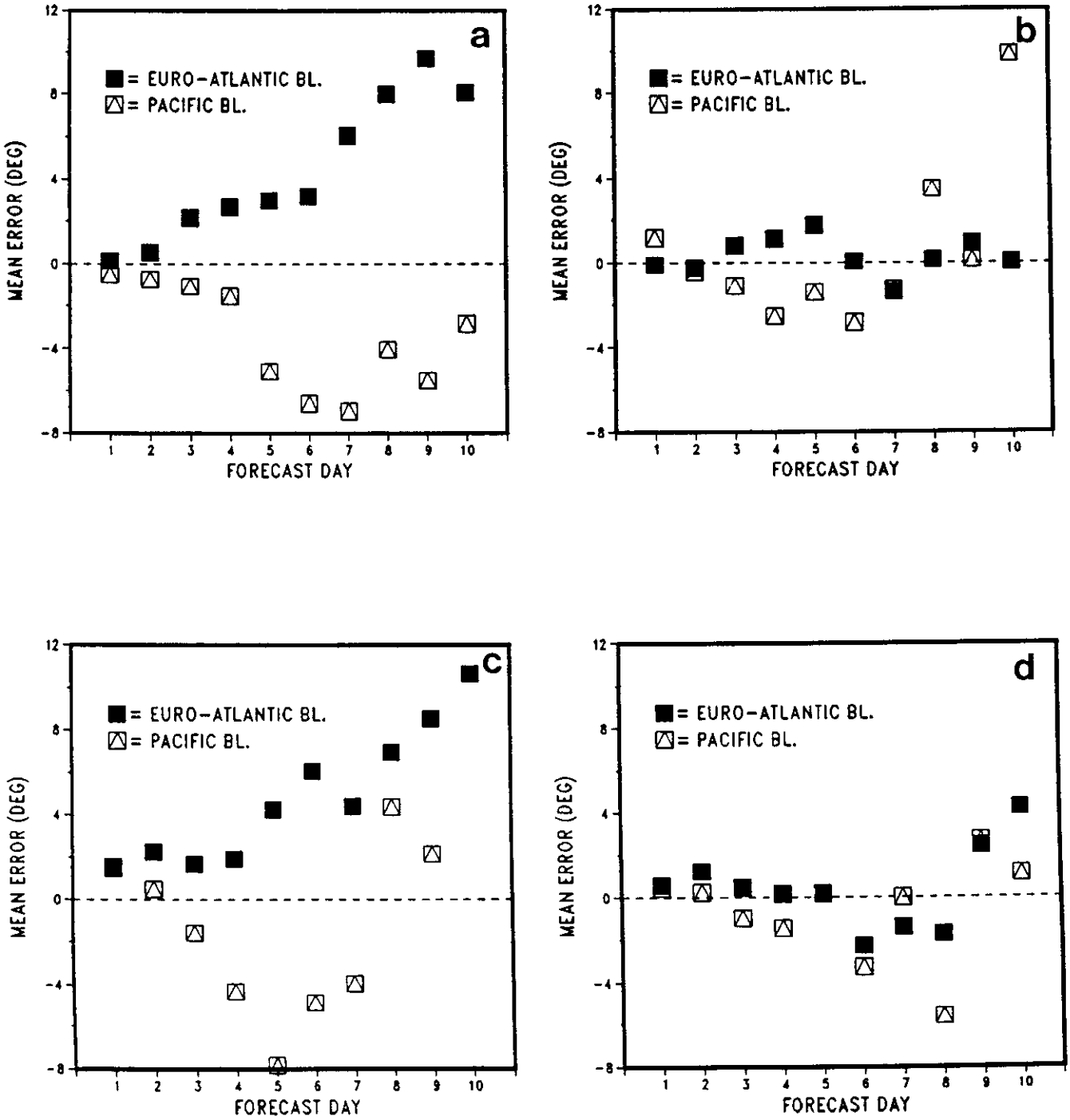
a
b
c
d
■ = EURO-ATLANTIC BL.
△ = PACIFIC BL.
MEAN ERROR (DEG)
FORECAST DAY
12
8
4
0
-4
-8
1
2
3
4
5
6
7
8
9
10

Fig 8

FORECAST OF BLOCKING ONSET – FIRST DAY OF EURO–ATLANTIC BL.

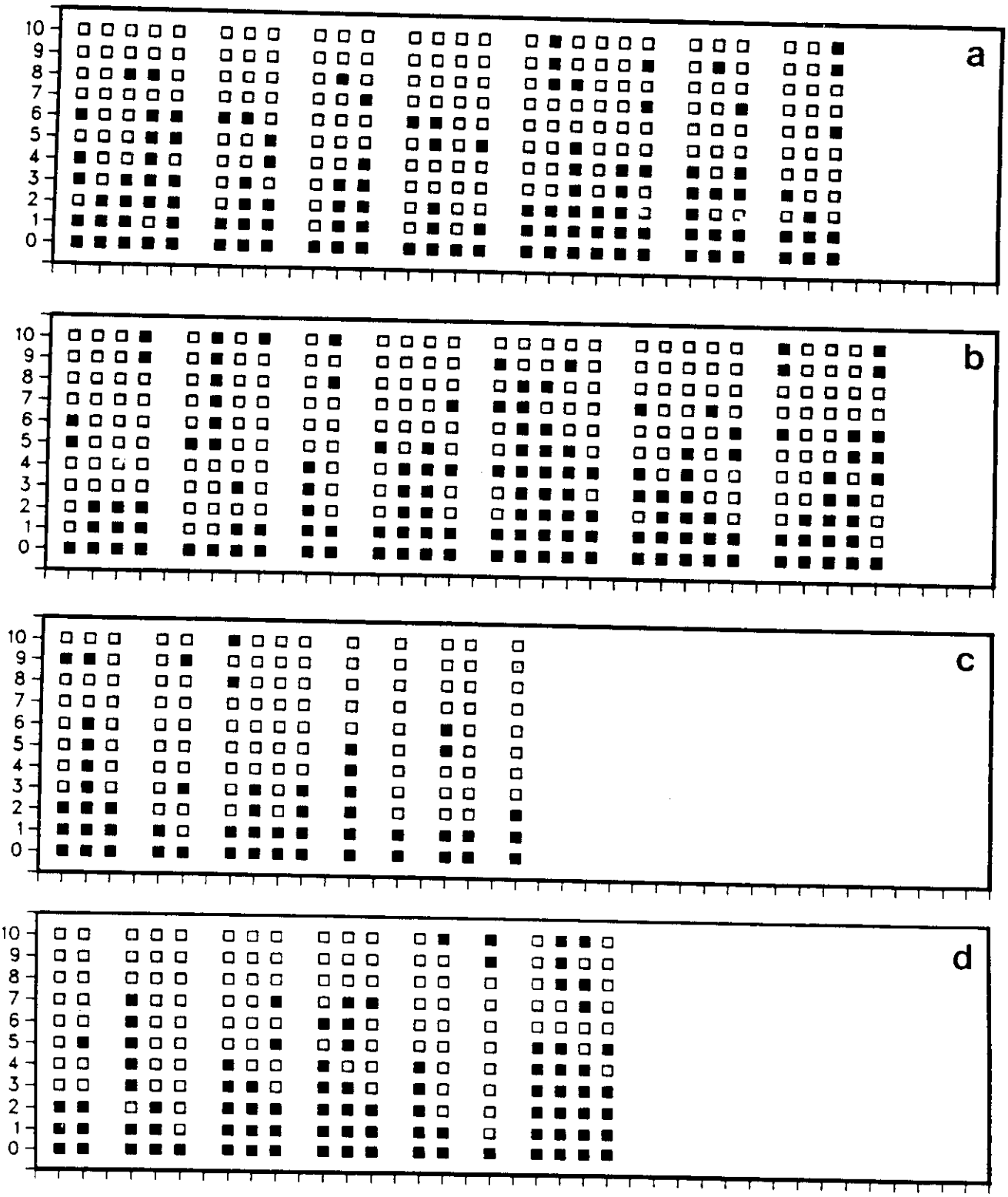

BLOCKING CASES

Fig 9

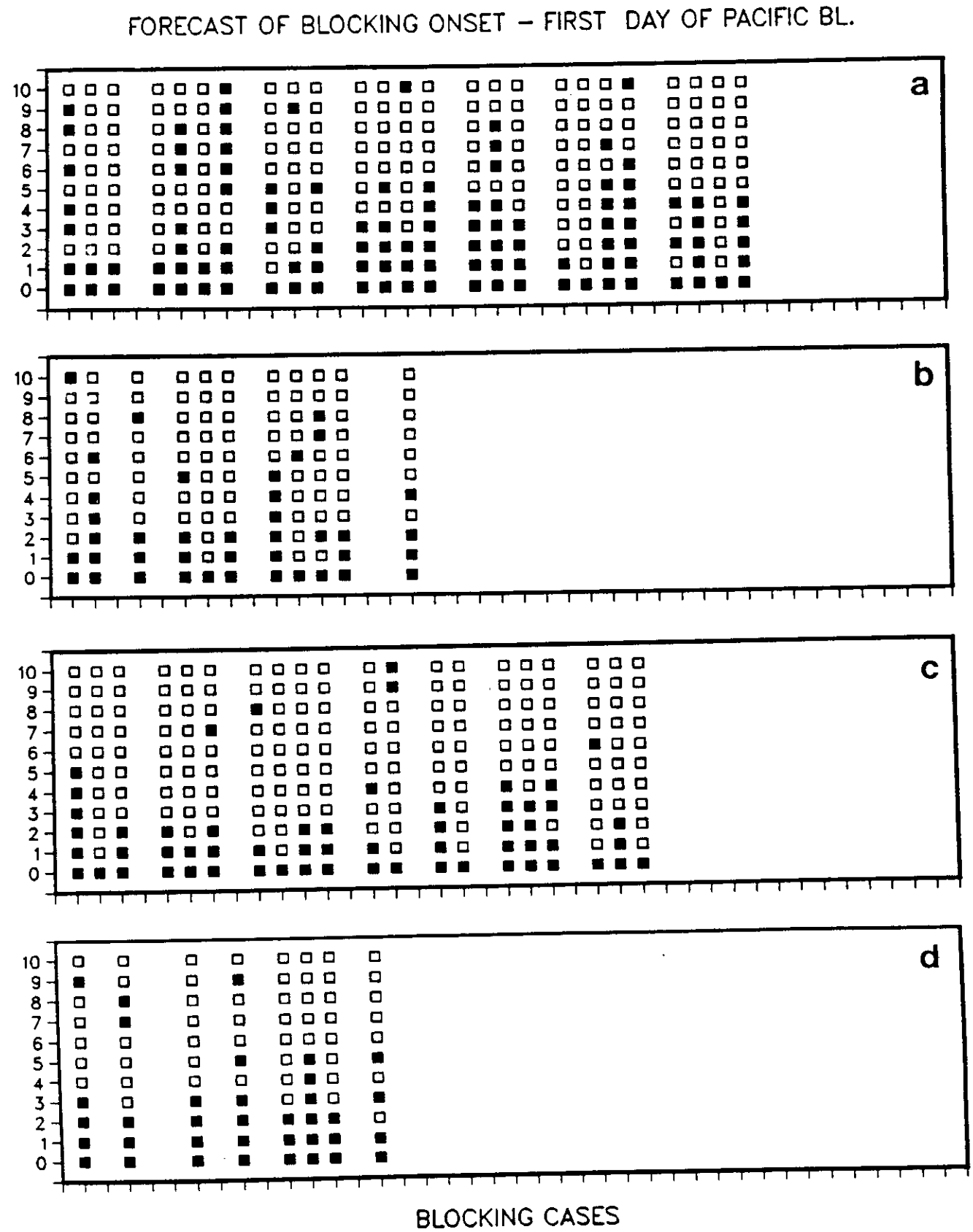
FORECAST OF BLOCKING ONSET – FIRST DAY OF PACIFIC BL.
a
b
c
d
10
9
8
7
6
5
4
3
2
1
0
BLOCKING CASES

Fig 10

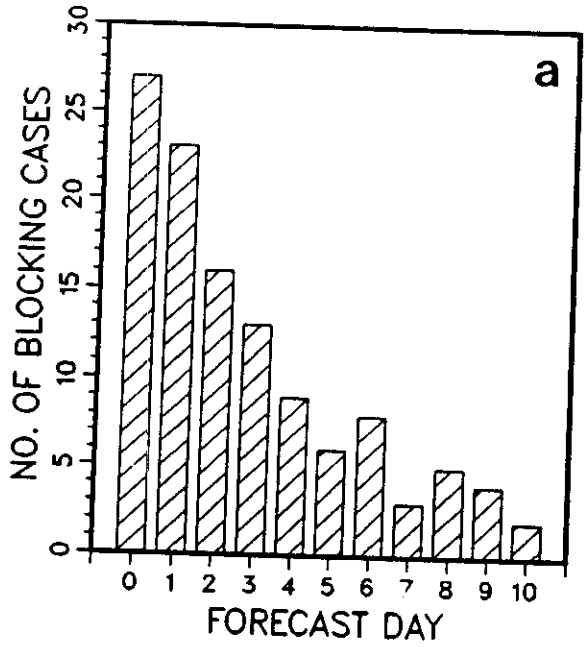
a
NO. OF BLOCKING CASES
0 5 10 15 20 25 30
0 1 2 3 4 5 6 7 8 9 10
FORECAST DAY

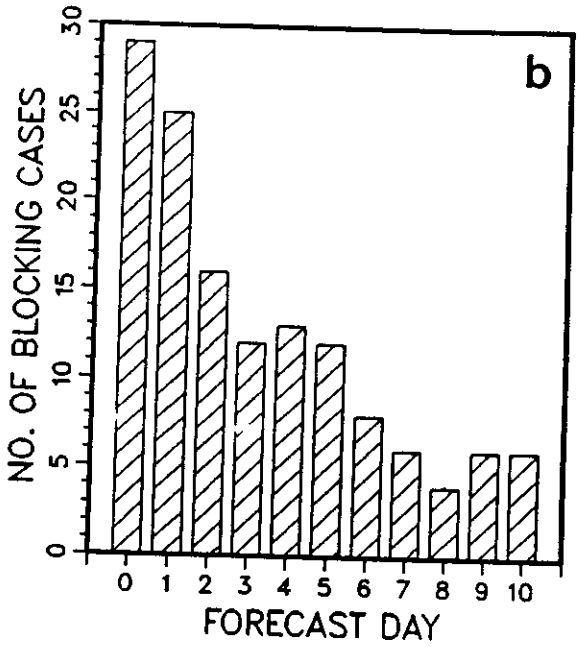
b
NO. OF BLOCKING CASES
0 5 10 15 20 25 30
0 1 2 3 4 5 6 7 8 9 10
FORECAST DAY

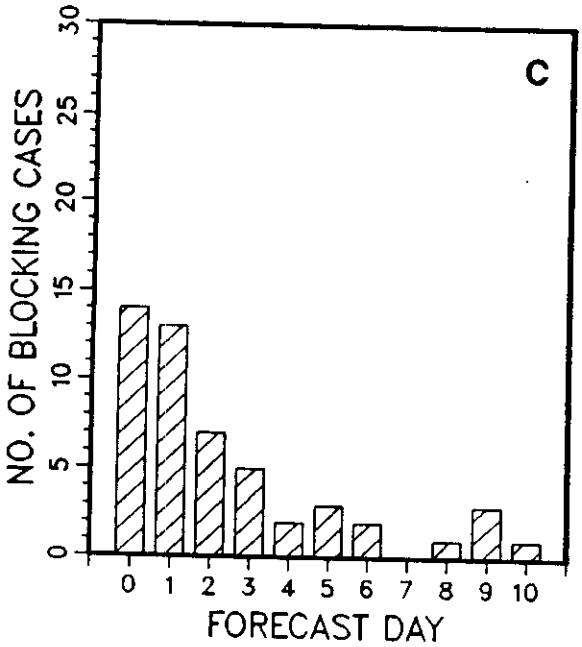
c
NO. OF BLOCKING CASES
0 5 10 15 20 25 30
0 1 2 3 4 5 6 7 8 9 10
FORECAST DAY

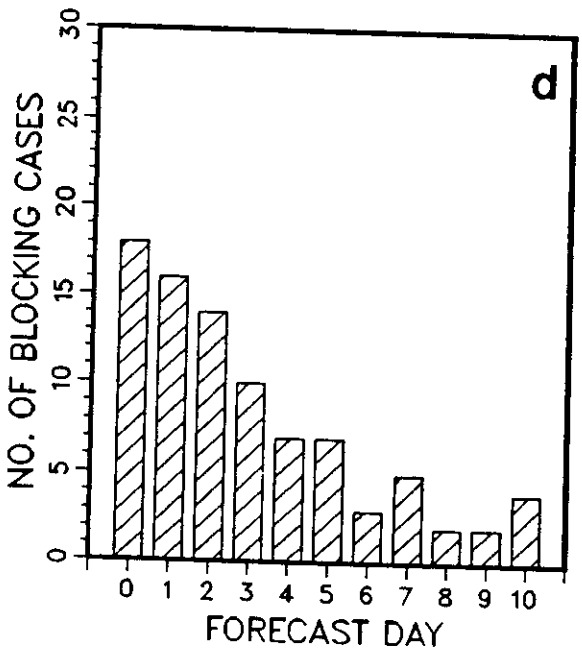
d
NO. OF BLOCKING CASES
0 5 10 15 20 25 30
0 1 2 3 4 5 6 7 8 9 10
FORECAST DAY

Fig 11

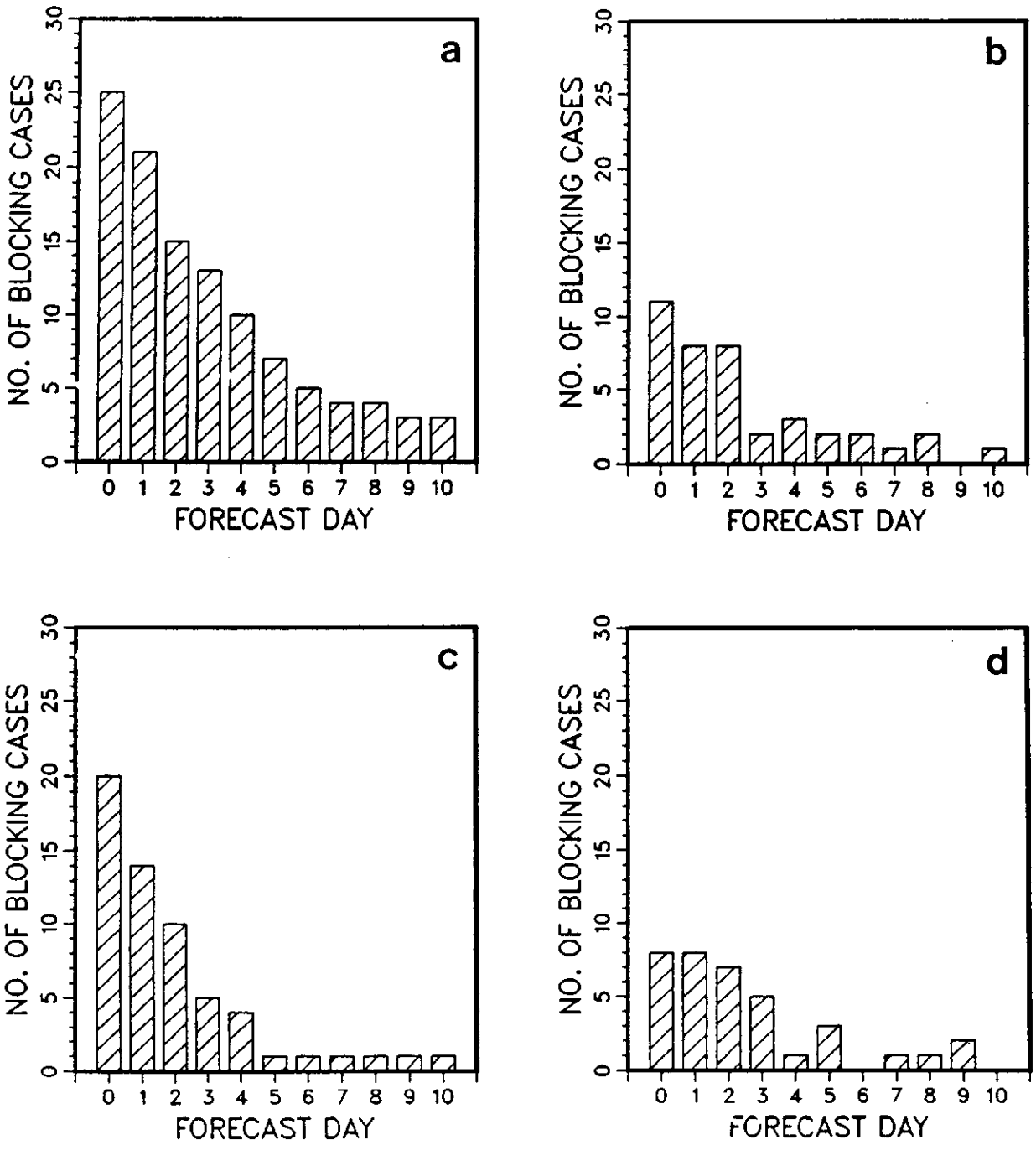
a
b
c
d
NO. OF BLOCKING CASES
FORECAST DAY
0 1 2 3 4 5 6 7 8 9 10
0 5 10 15 20 25 30

Fig 12

FORECAST OF BLOCKING DURATION – EURO–ATLANTIC BL.

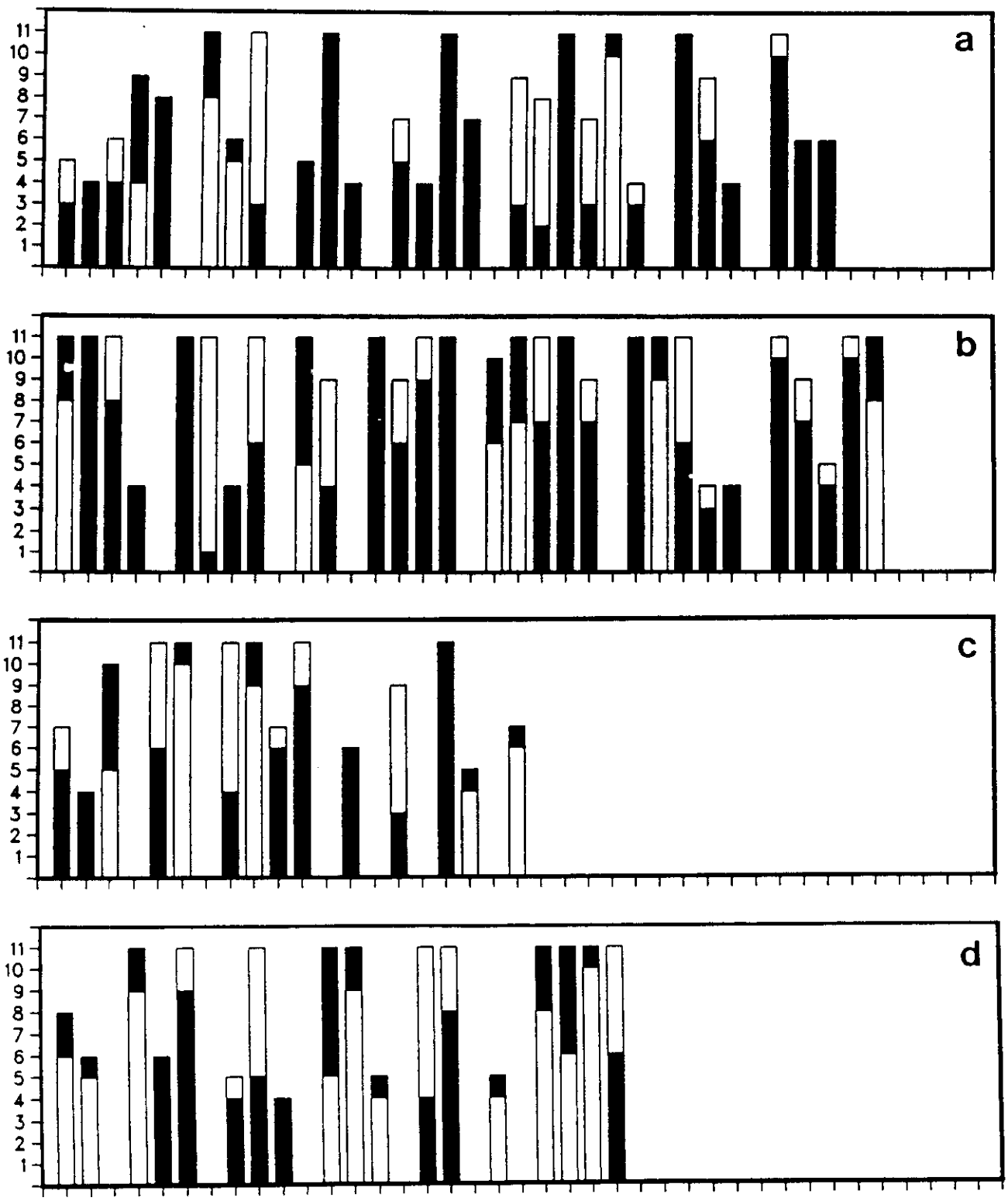

Fig 13

FORECAST OF BLOCKING DURATION – PACIFIC BL.

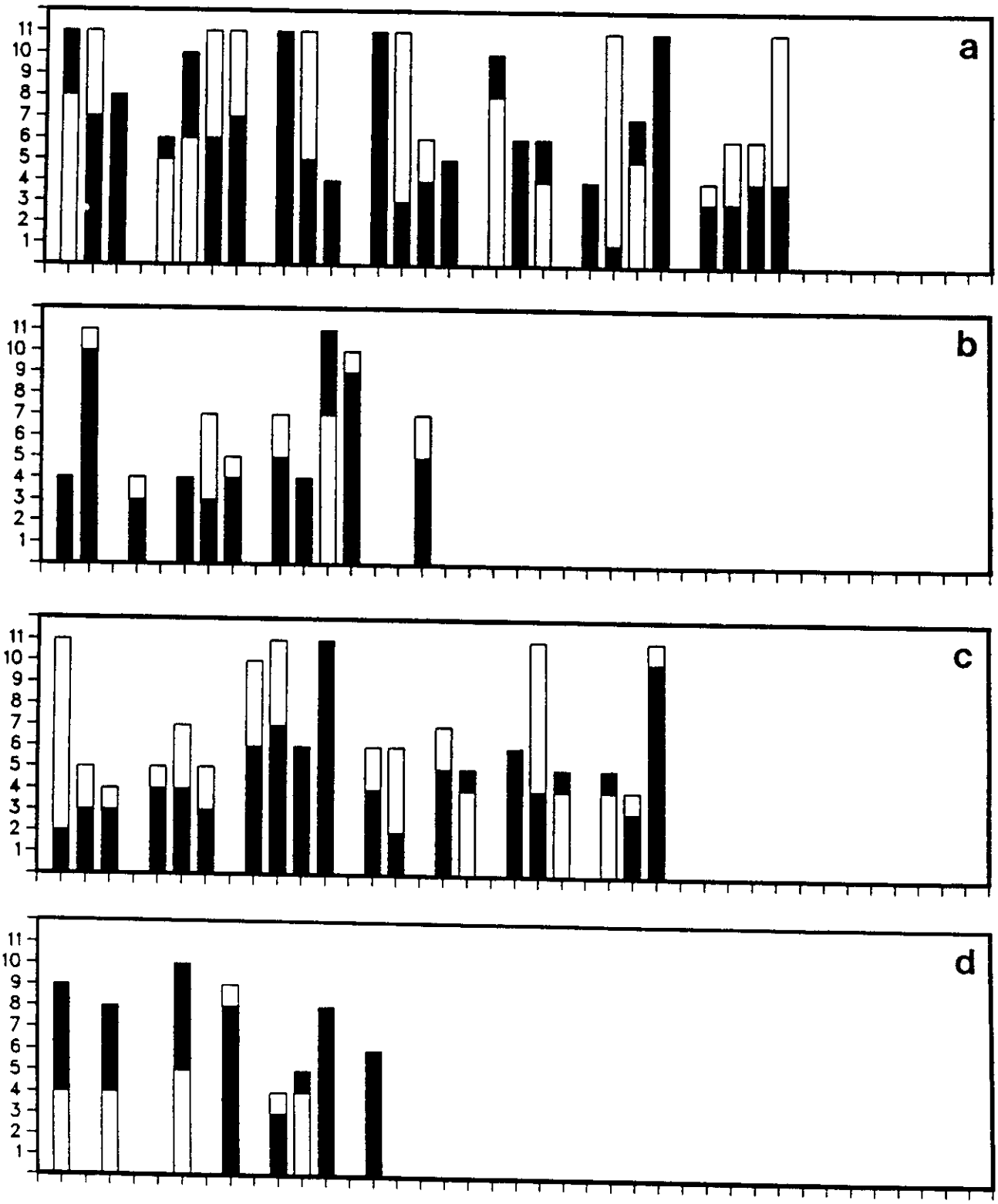

BLOCKING CASES

Fig 14

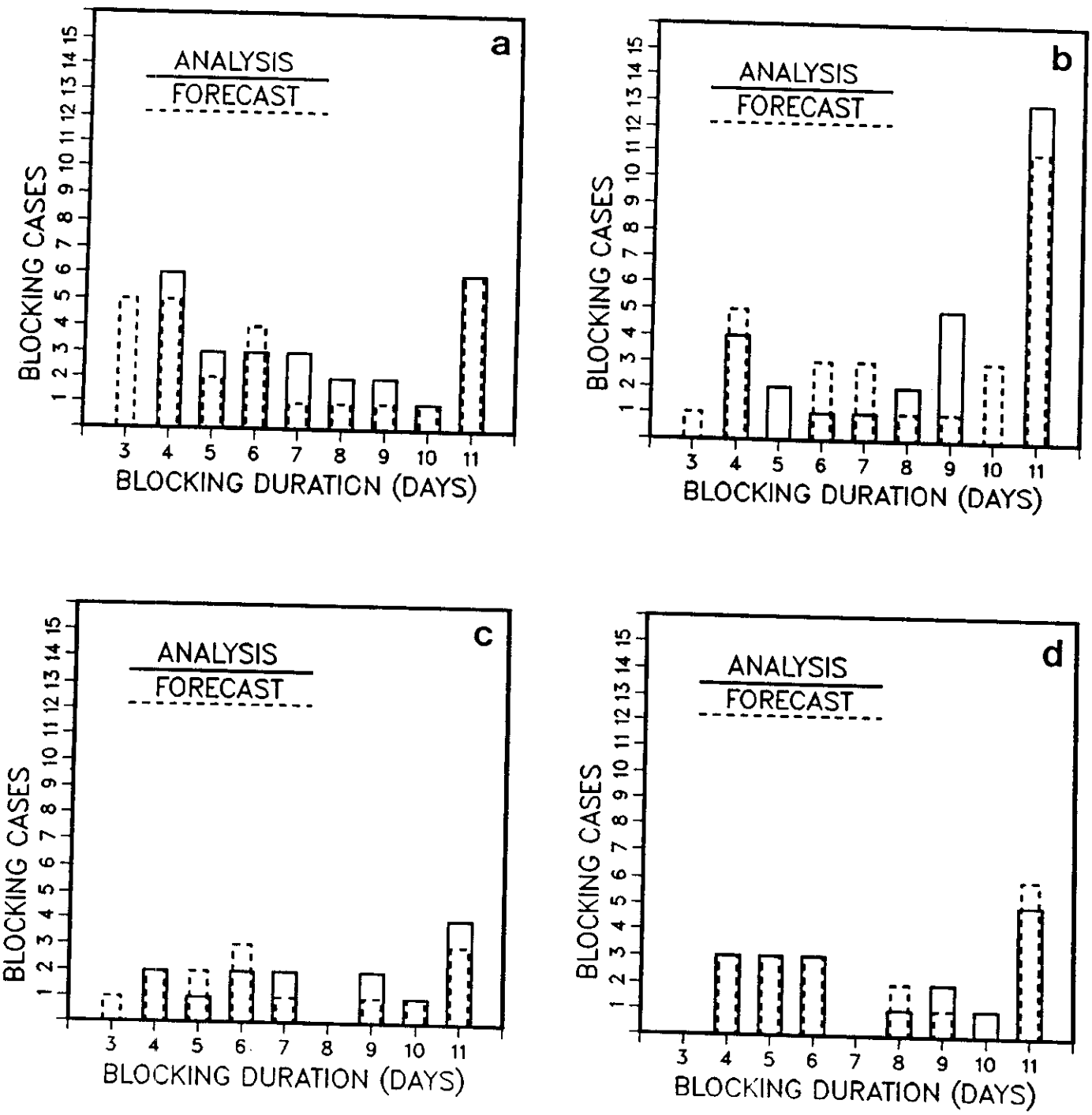
a
ANALYSIS
FORECAST
BLOCKING CASES
1 2 3 4 5 6 7 8 9 10 11 12 13 14 15
3 4 5 6 7 8 9 10 11
BLOCKING DURATION (DAYS)
b
ANALYSIS
FORECAST
BLOCKING CASES
1 2 3 4 5 6 7 8 9 10 11 12 13 14 15
3 4 5 6 7 8 9 10 11
BLOCKING DURATION (DAYS)
c
ANALYSIS
FORECAST
BLOCKING CASES
1 2 3 4 5 6 7 8 9 10 11 12 13 14 15
3 4 5 6 7 8 9 10 11
BLOCKING DURATION (DAYS)
d
ANALYSIS
FORECAST
BLOCKING CASES
1 2 3 4 5 6 7 8 9 10 11 12 13 14 15
3 4 5 6 7 8 9 10 11
BLOCKING DURATION (DAYS)

Fig 15

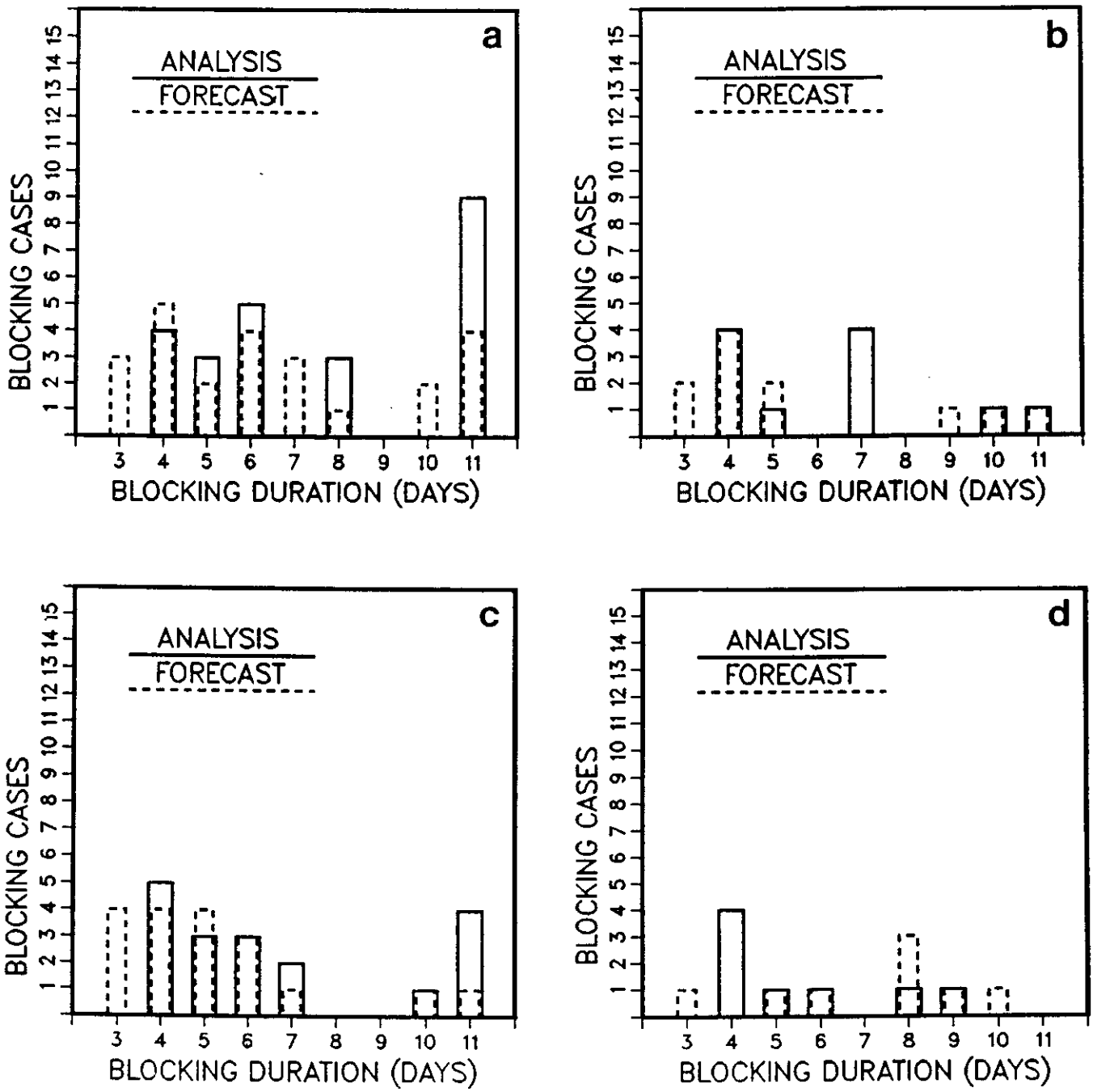
a
ANALYSIS
FORECAST
BLOCKING CASES
1 2 3 4 5 6 7 8 9 10 11 12 13 14 15
3 4 5 6 7 8 9 10 11
BLOCKING DURATION (DAYS)
b
ANALYSIS
FORECAST
BLOCKING CASES
1 2 3 4 5 6 7 8 9 10 11 12 13 14 15
3 4 5 6 7 8 9 10 11
BLOCKING DURATION (DAYS)
c
ANALYSIS
FORECAST
BLOCKING CASES
1 2 3 4 5 6 7 8 9 10 11 12 13 14 15
3 4 5 6 7 8 9 10 11
BLOCKING DURATION (DAYS)
d
ANALYSIS
FORECAST
BLOCKING CASES
1 2 3 4 5 6 7 8 9 10 11 12 13 14 15
3 4 5 6 7 8 9 10 11
BLOCKING DURATION (DAYS)

Fig 16

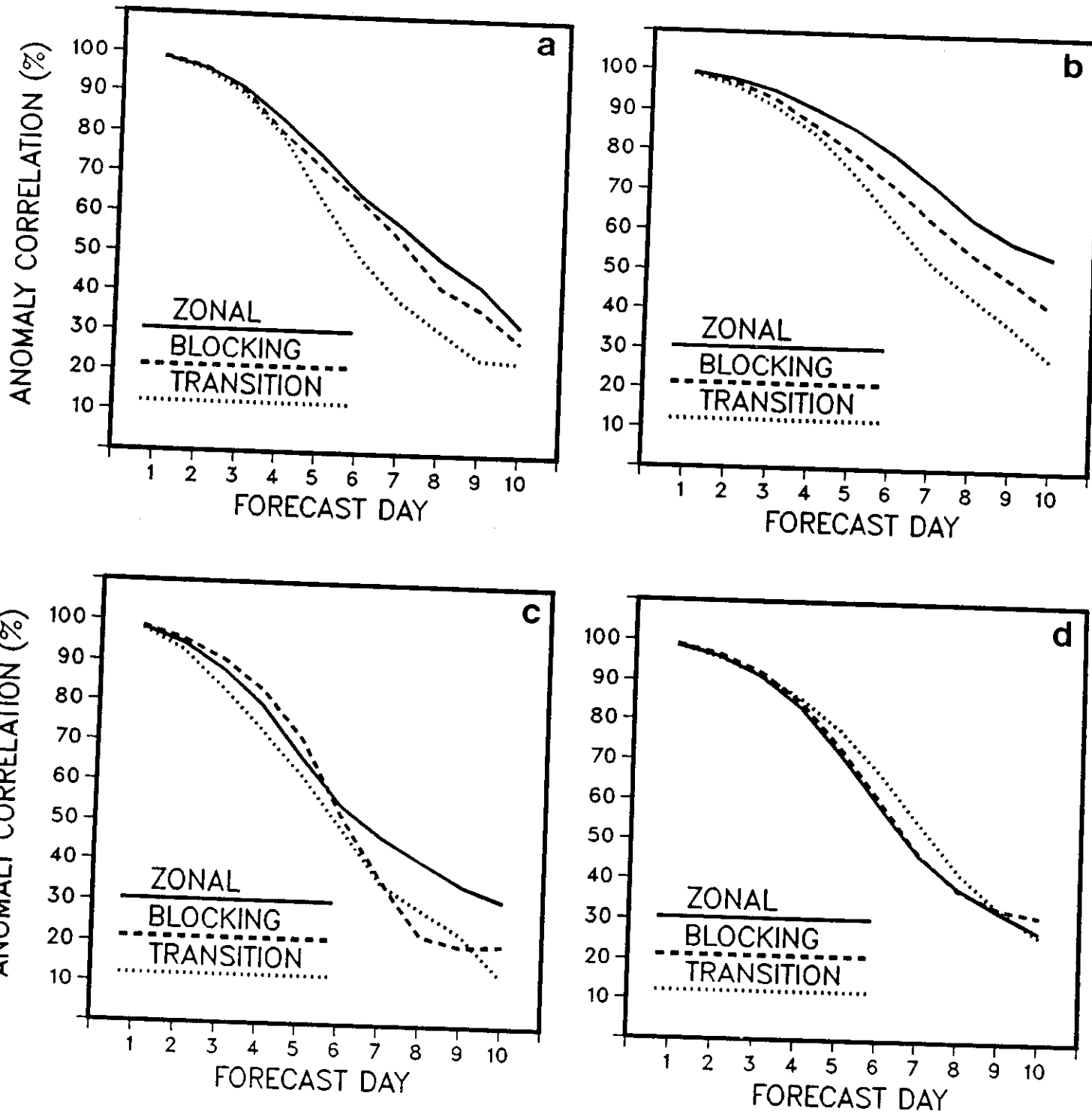
a
b
c
d
ANOMALY CORRELATION (%)
FORECAST DAY
ZONAL
BLOCKING
TRANSITION
100
90
80
70
60
50
40
30
20
10
1 2 3 4 5 6 7 8 9 10

Fig 17

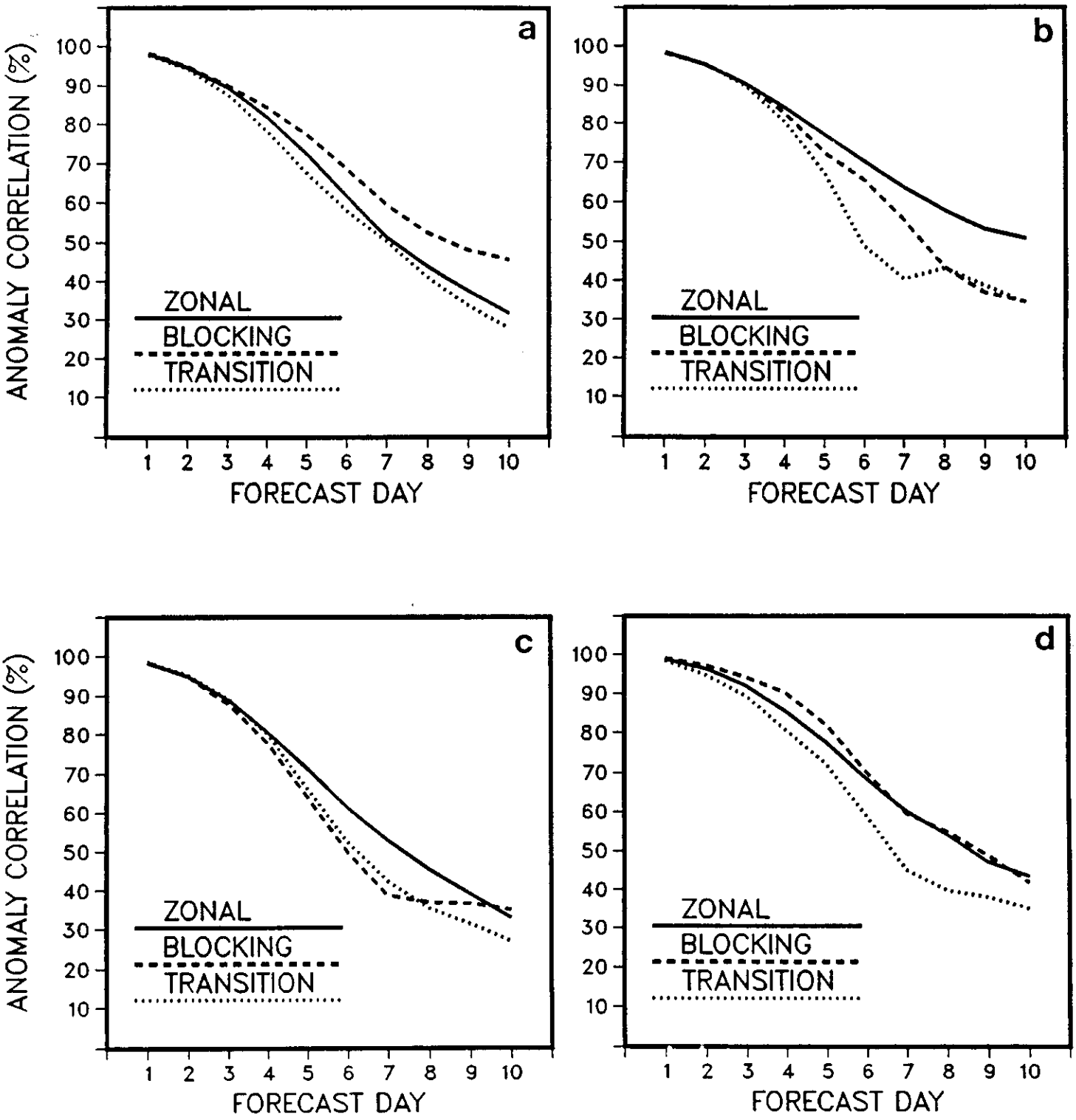
a
b
c
d
ANOMALY CORRELATION (%)
100
90
80
70
60
50
40
30
20
10
1 2 3 4 5 6 7 8 9 10
FORECAST DAY
ZONAL
BLOCKING
TRANSITION

Fig 18

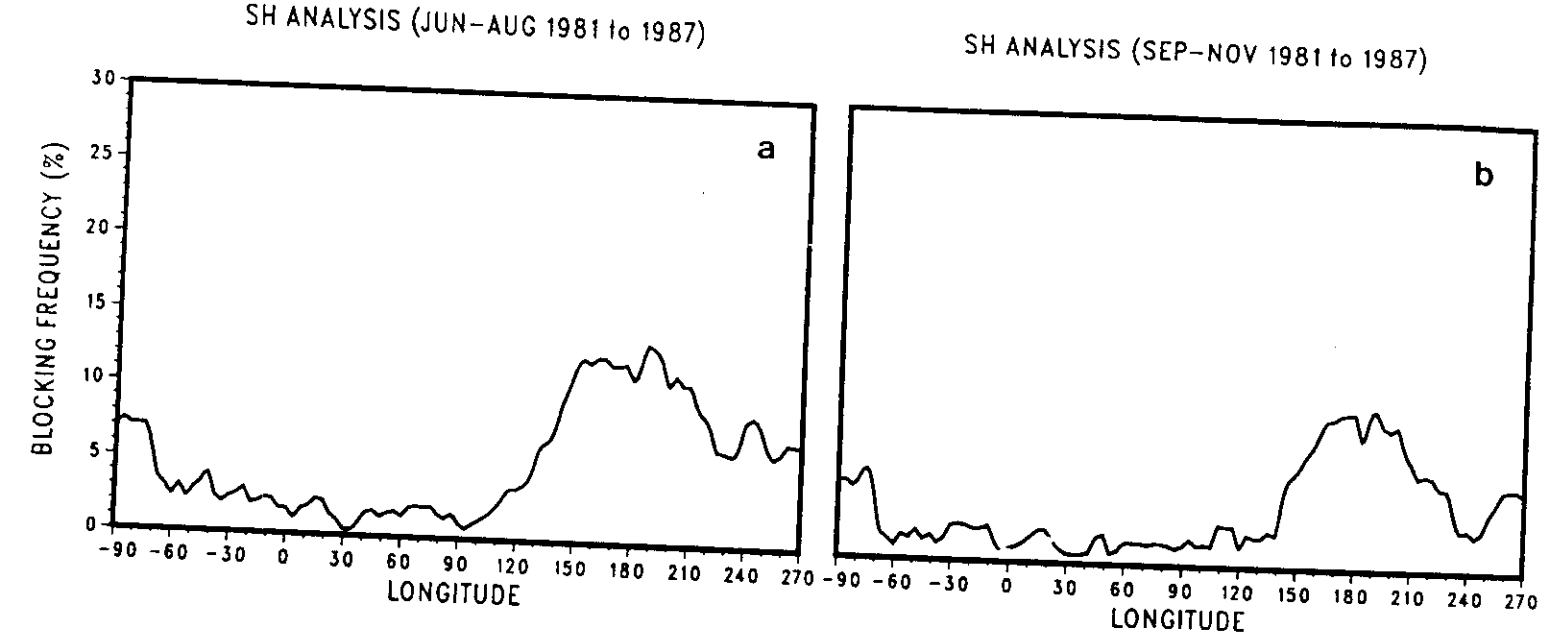
SH ANALYSIS (JUN–AUG 1981 to 1987)
SH ANALYSIS (SEP–NOV 1981 to 1987)
BLOCKING FREQUENCY (%)
a
b
LONGITUDE
LONGITUDE

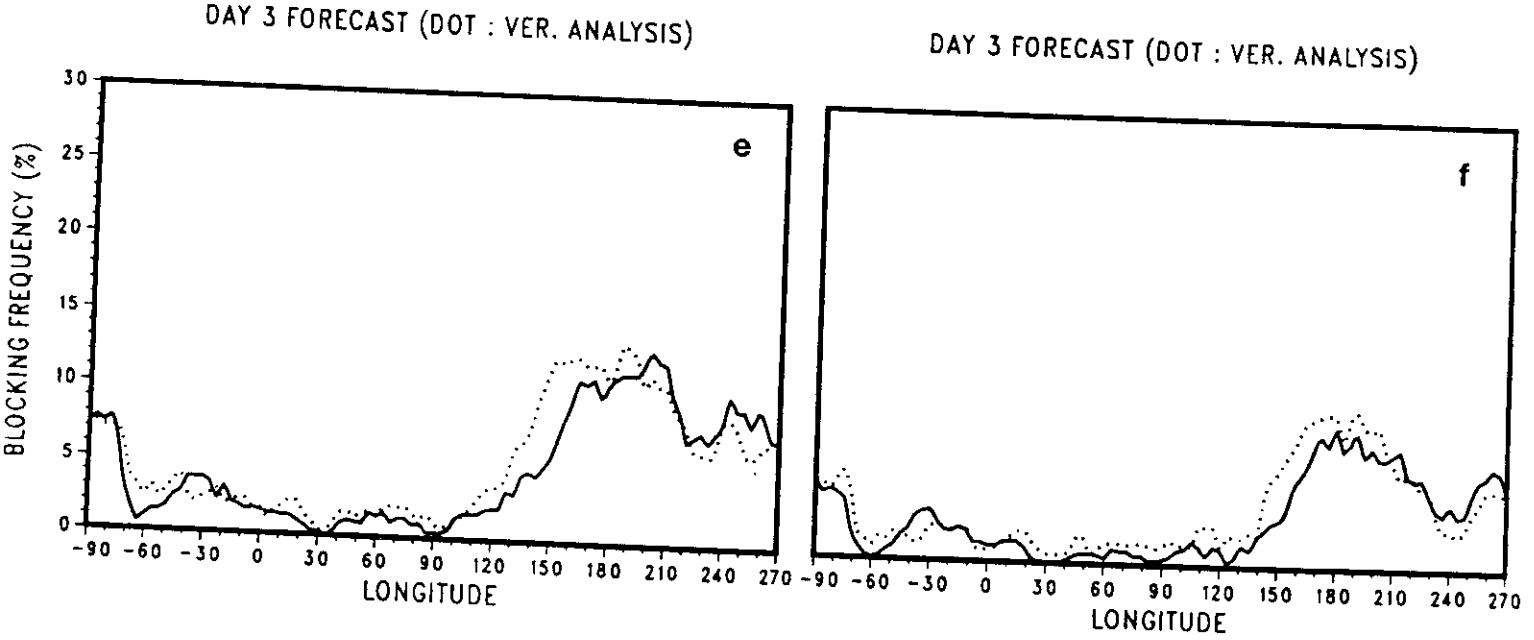
DAY 3 FORECAST (DOT : VER. ANALYSIS)
DAY 3 FORECAST (DOT : VER. ANALYSIS)
BLOCKING FREQUENCY (%)
e
f
LONGITUDE
LONGITUDE

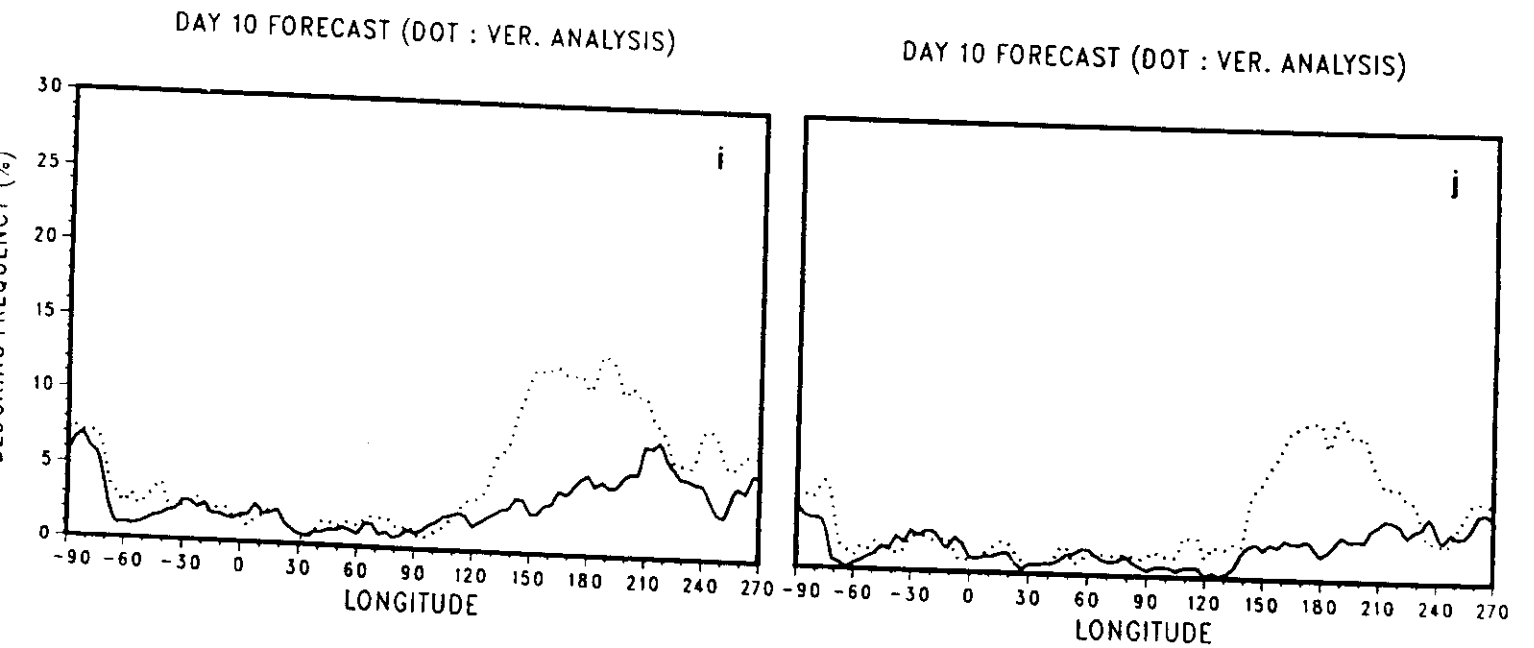
DAY 10 FORECAST (DOT : VER. ANALYSIS)
DAY 10 FORECAST (DOT : VER. ANALYSIS)
i
j
LONGITUDE
LONGITUDE

Fig-19 I

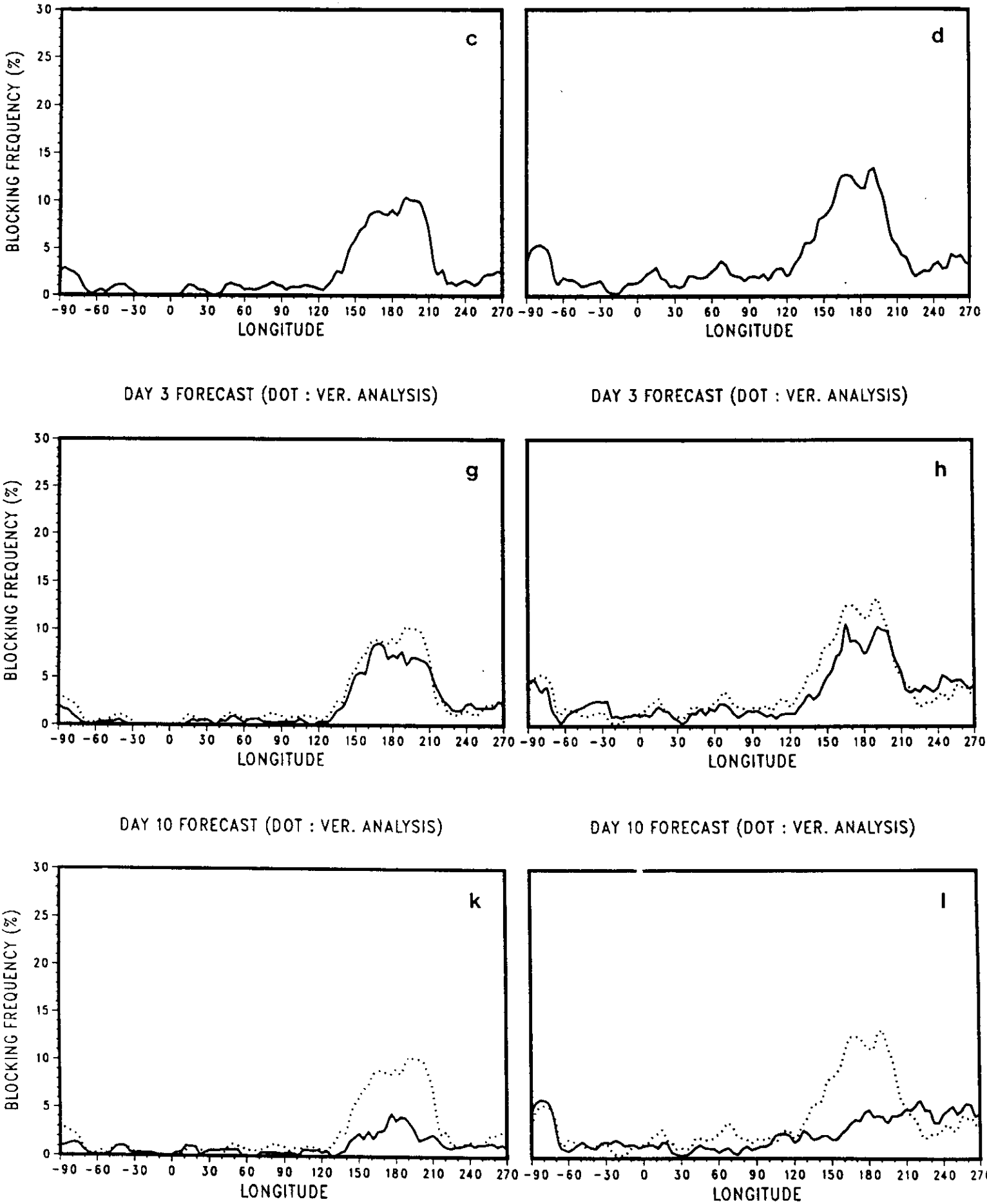
SH ANALYSIS (DEC–FEB 1981 to 1987)
SH ANALYSIS (MAR–MAY 1981 to 1987)
c
d
BLOCKING FREQUENCY (%)
LONGITUDE
DAY 3 FORECAST (DOT : VER. ANALYSIS)
DAY 3 FORECAST (DOT : VER. ANALYSIS)
g
h
DAY 10 FORECAST (DOT : VER. ANALYSIS)
DAY 10 FORECAST (DOT : VER. ANALYSIS)
k
l
-90 -60 -30 0 30 60 90 120 150 180 210 240 270
0 5 10 15 20 25 30

Fig 19 cont

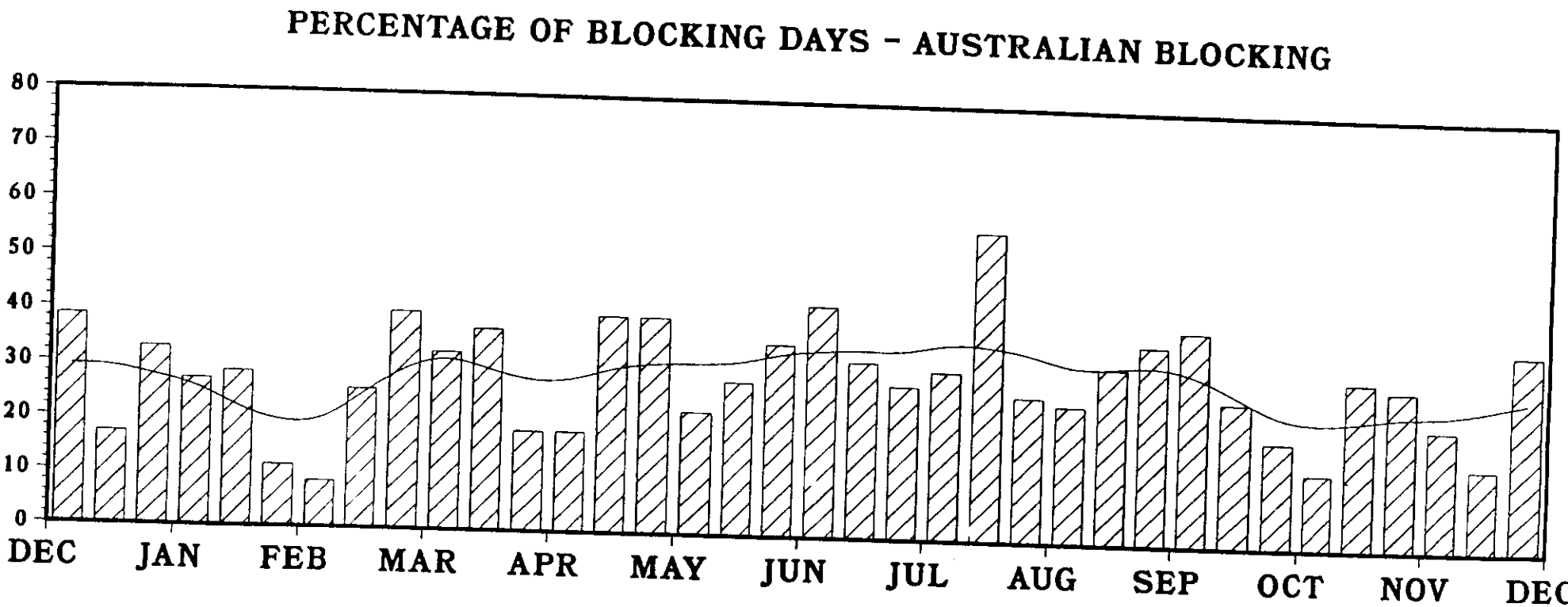
PERCENTAGE OF BLOCKING DAYS - AUSTRALIAN BLOCKING
80
70
60
50
40
30
20
10
0
DEC
JAN
FEB
MAR
APR
MAY
JUN
JUL
AUG
SEP
OCT
NOV
DEC

Fig 20

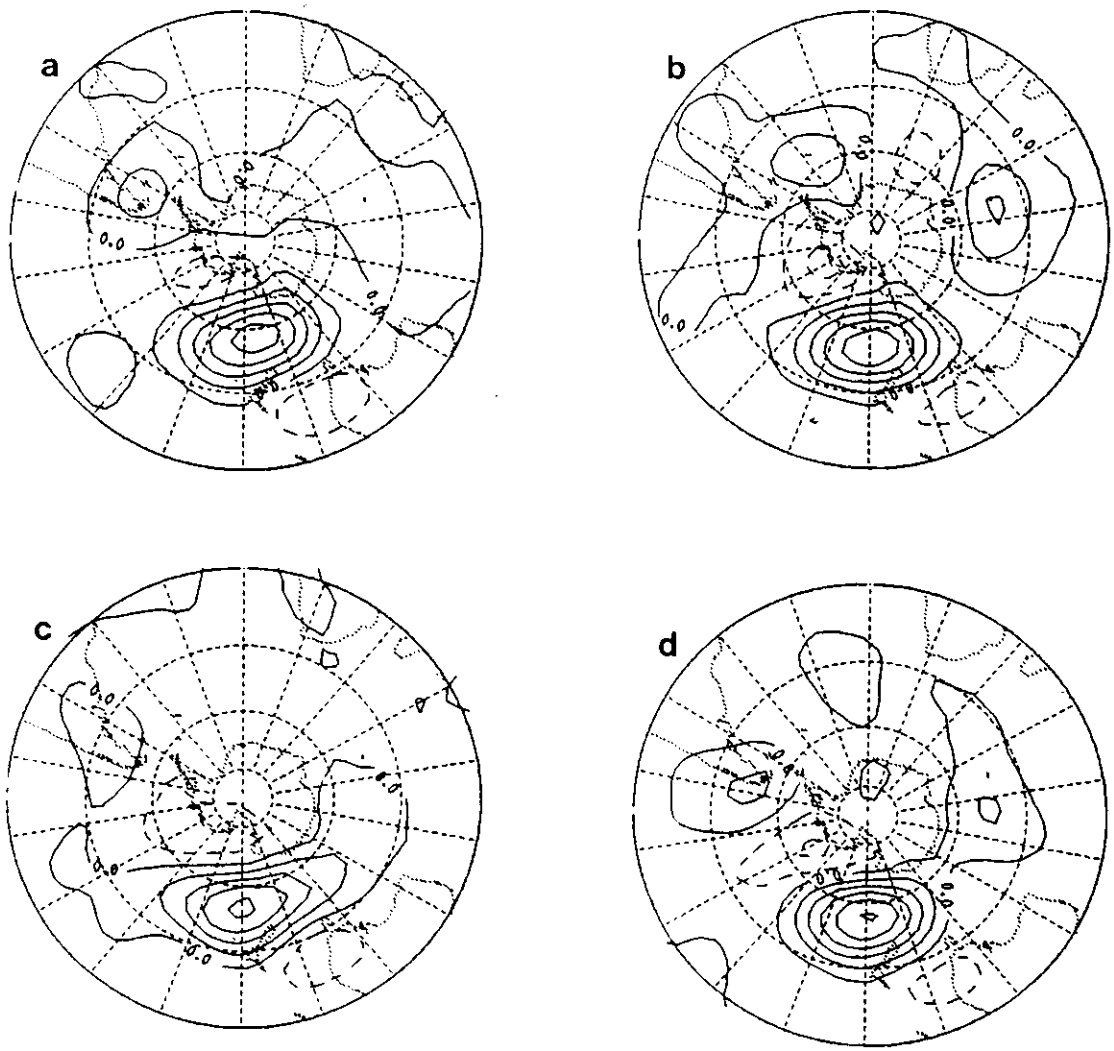

Fig 21

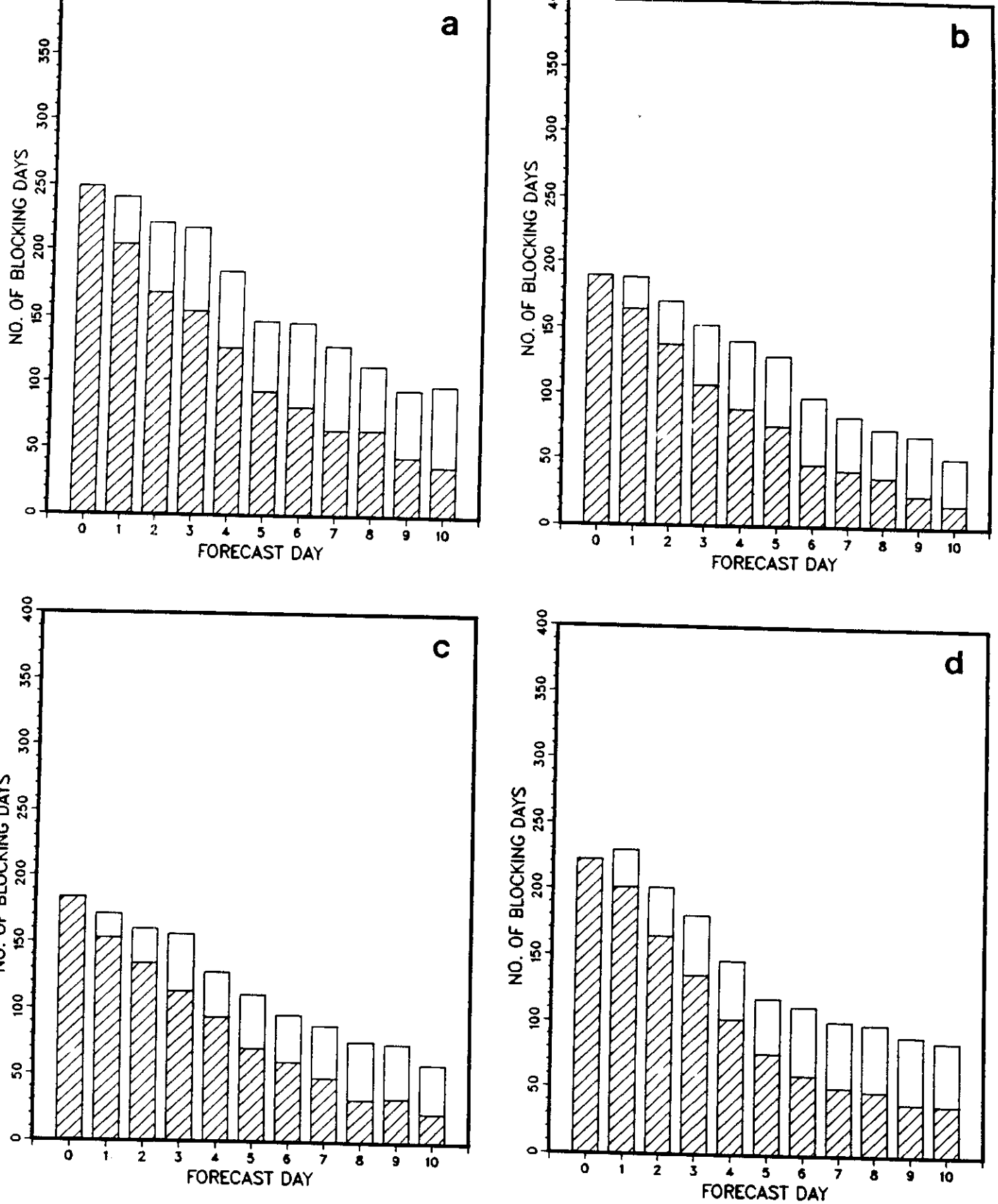
a
b
c
d
NO. OF BLOCKING DAYS
FORECAST DAY
0
50
100
150
200
250
300
350
400
0 1 2 3 4 5 6 7 8 9 10

Fig 22

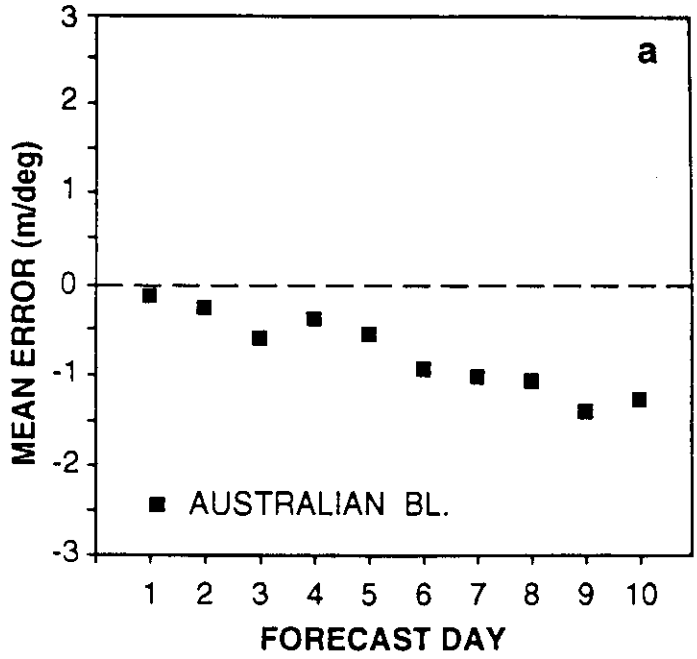
a
MEAN ERROR (m/deg)
3
2
1
0
-1
-2
-3
AUSTRALIAN BL.
1 2 3 4 5 6 7 8 9 10
FORECAST DAY

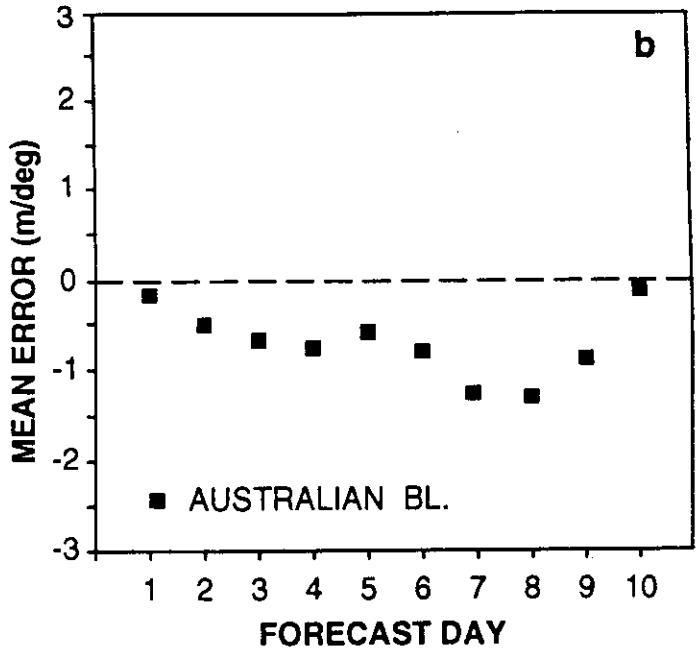
b
MEAN ERROR (m/deg)
3
2
1
0
-1
-2
-3
AUSTRALIAN BL.
1 2 3 4 5 6 7 8 9 10
FORECAST DAY

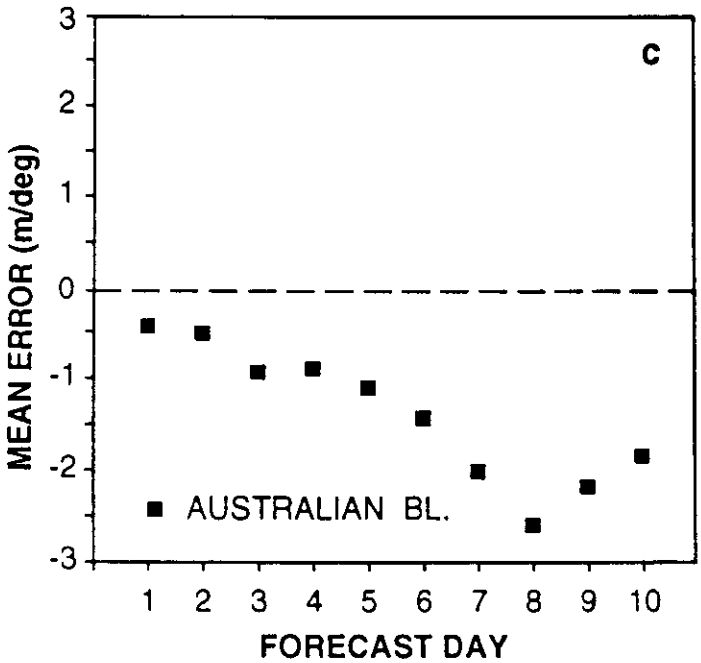
c
MEAN ERROR (m/deg)
3
2
1
0
-1
-2
-3
AUSTRALIAN BL.
1 2 3 4 5 6 7 8 9 10
FORECAST DAY

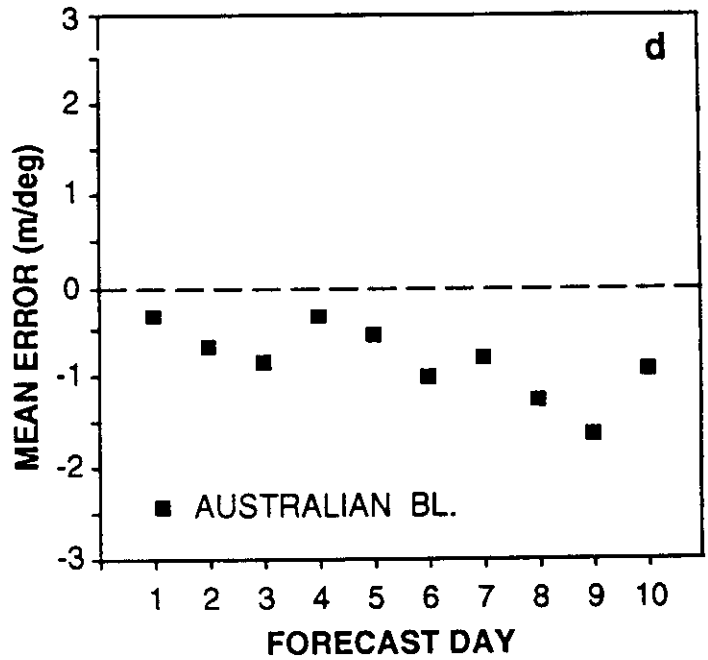
d
MEAN ERROR (m/deg)
3
2
1
0
-1
-2
-3
AUSTRALIAN BL.
1 2 3 4 5 6 7 8 9 10
FORECAST DAY

Fig 23

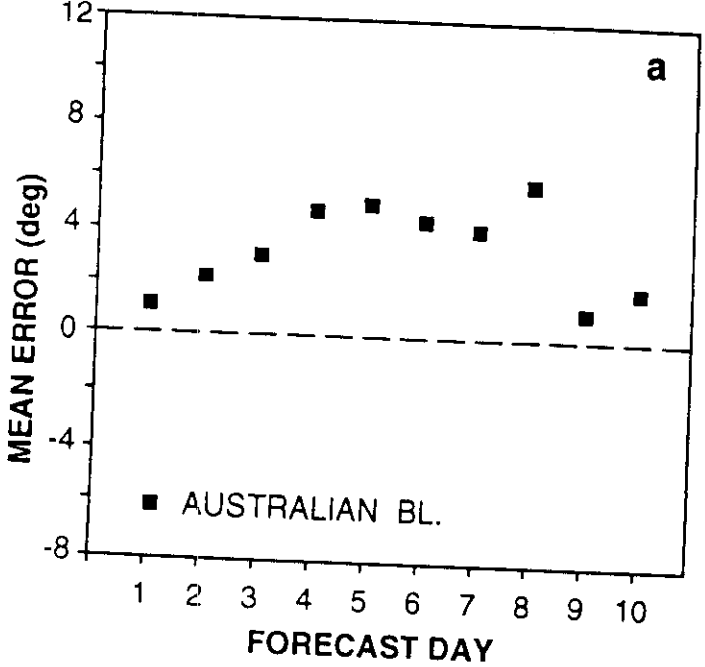
a
MEAN ERROR (deg)
12
8
4
0
-4
-8
AUSTRALIAN BL.
1 2 3 4 5 6 7 8 9 10
FORECAST DAY

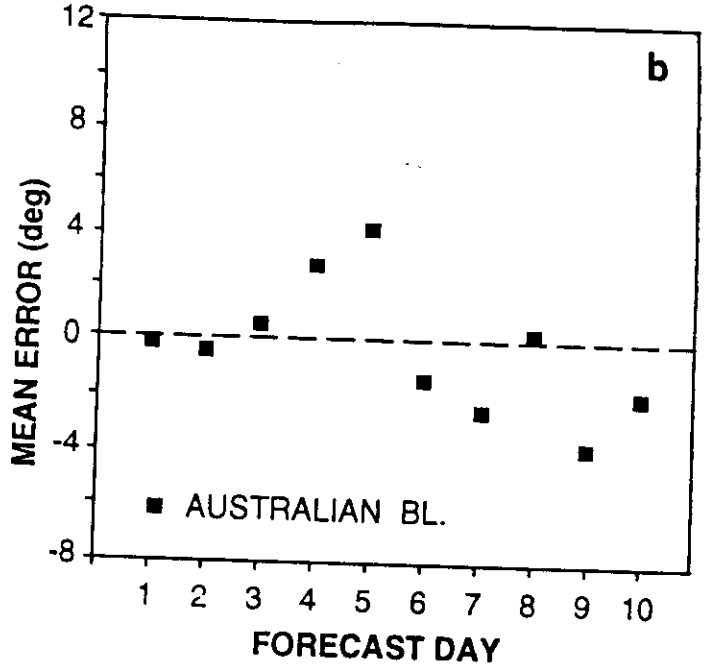
b
MEAN ERROR (deg)
12
8
4
0
-4
-8
AUSTRALIAN BL.
1 2 3 4 5 6 7 8 9 10
FORECAST DAY

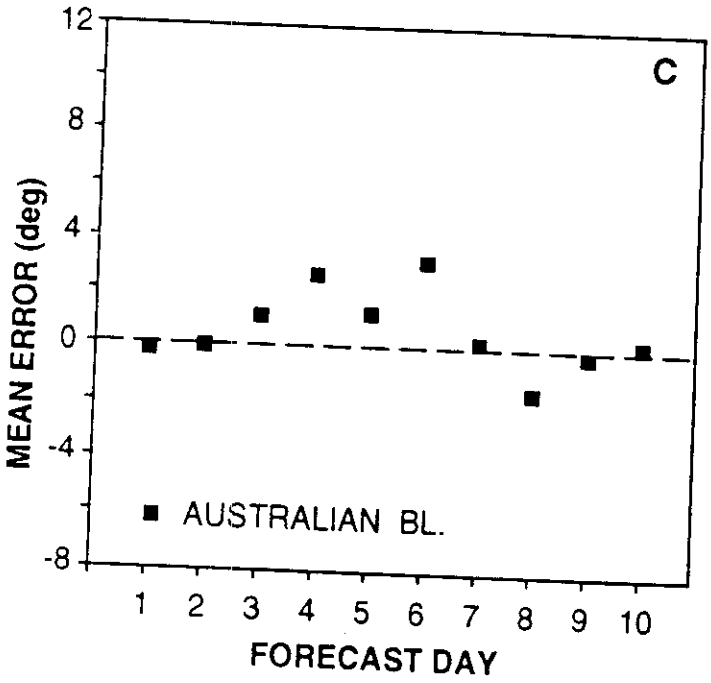
C
MEAN ERROR (deg)
12
8
4
0
-4
-8
AUSTRALIAN BL.
1 2 3 4 5 6 7 8 9 10
FORECAST DAY

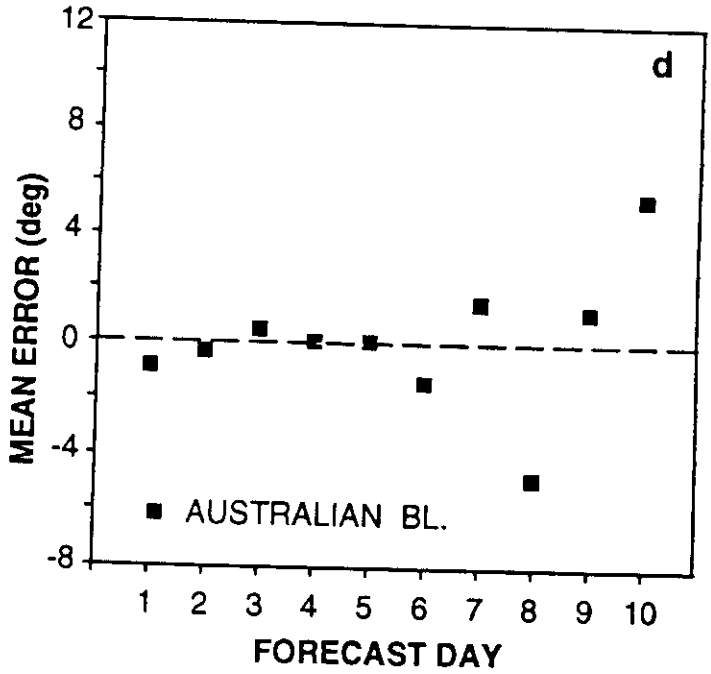
d
MEAN ERROR (deg)
12
8
4
0
-4
-8
AUSTRALIAN BL.
1 2 3 4 5 6 7 8 9 10
FORECAST DAY

Fig 24

FORECAST OF BLOCKING ONSET – FIRST DAY OF AUSTRALIAN BL.

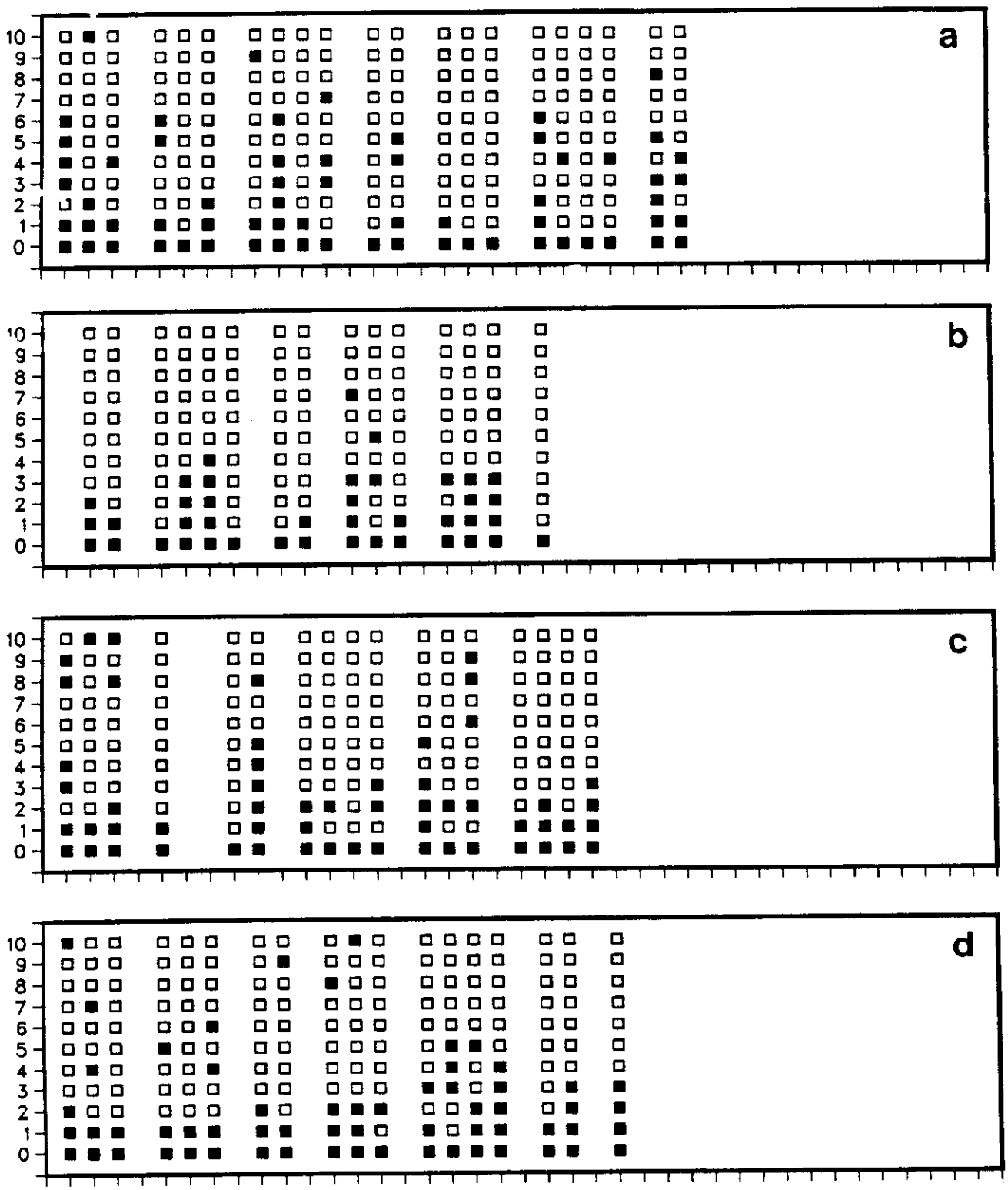

BLOCKING CASES

Fig 25

FORECAST OF BLOCKING DURATION – AUSTRALIAN BL.

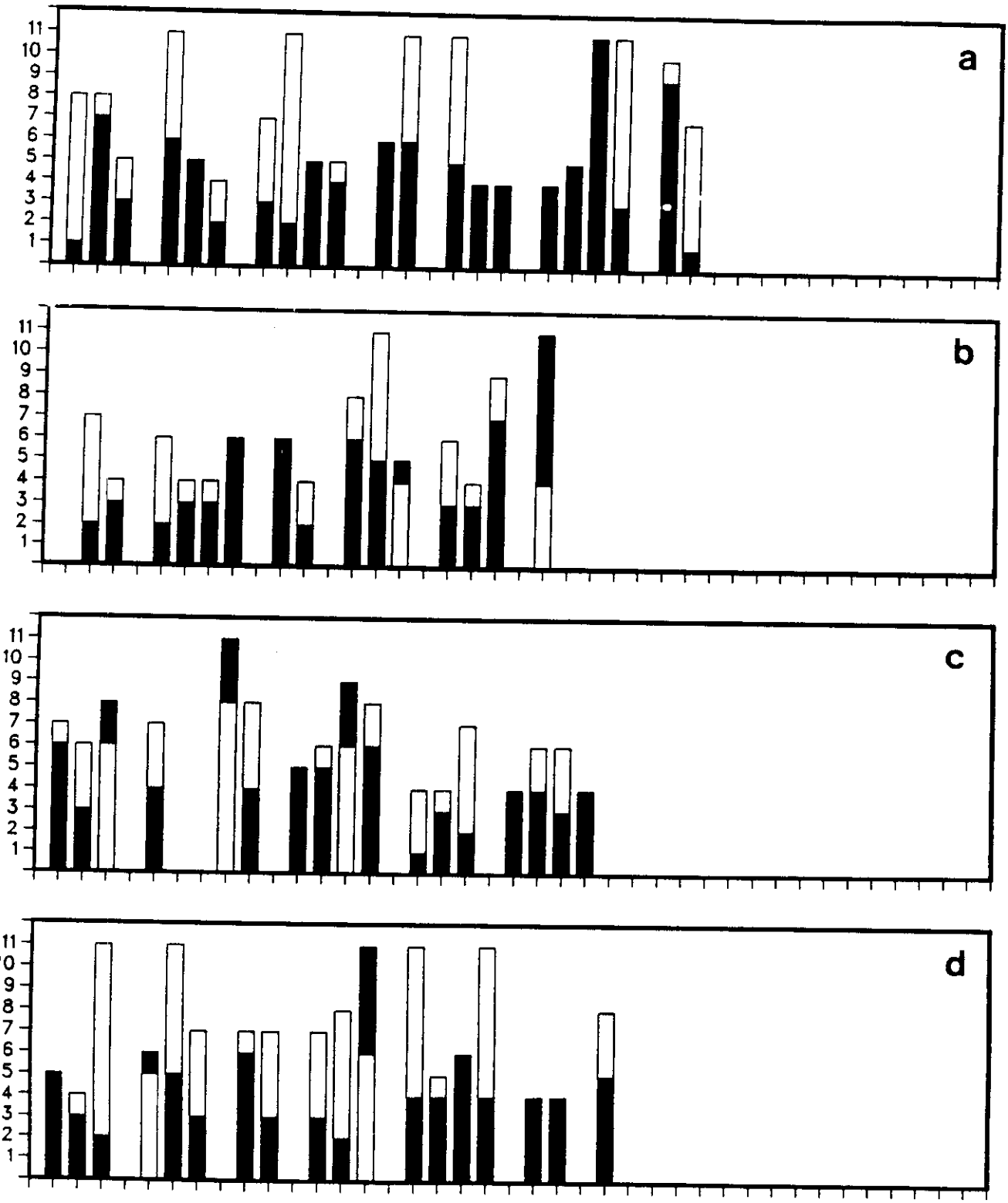

BLOCKING CASES

Fig 26

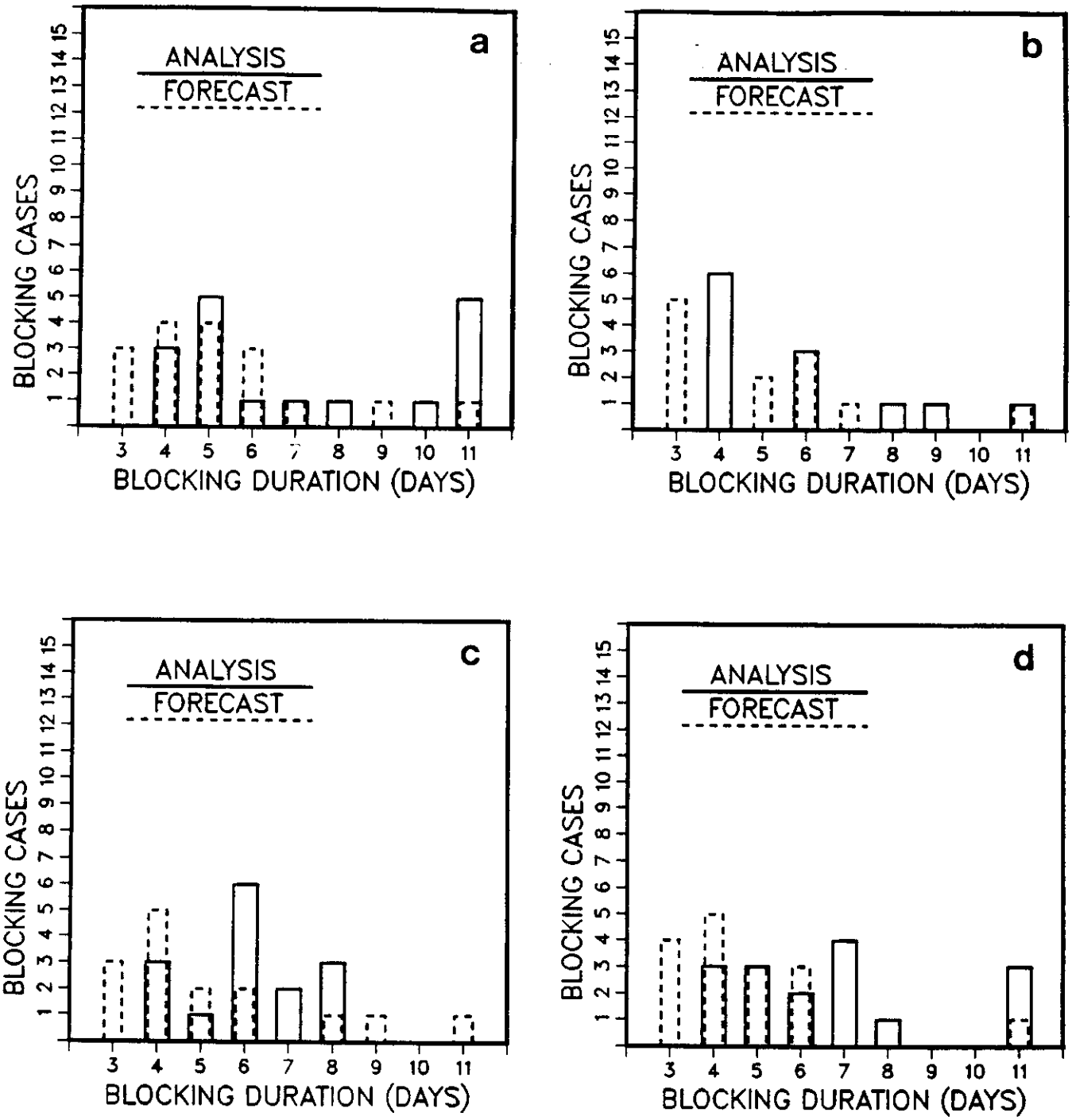
a
ANALYSIS
FORECAST
BLOCKING CASES
1 2 3 4 5 6 7 8 9 10 11 12 13 14 15
3 4 5 6 7 8 9 10 11
BLOCKING DURATION (DAYS)
b
ANALYSIS
FORECAST
BLOCKING CASES
1 2 3 4 5 6 7 8 9 10 11 12 13 14 15
3 4 5 6 7 8 9 10 11
BLOCKING DURATION (DAYS)
c
ANALYSIS
FORECAST
BLOCKING CASES
1 2 3 4 5 6 7 8 9 10 11 12 13 14 15
3 4 5 6 7 8 9 10 11
BLOCKING DURATION (DAYS)
d
ANALYSIS
FORECAST
BLOCKING CASES
1 2 3 4 5 6 7 8 9 10 11 12 13 14 15
3 4 5 6 7 8 9 10 11
BLOCKING DURATION (DAYS)

Fig 27

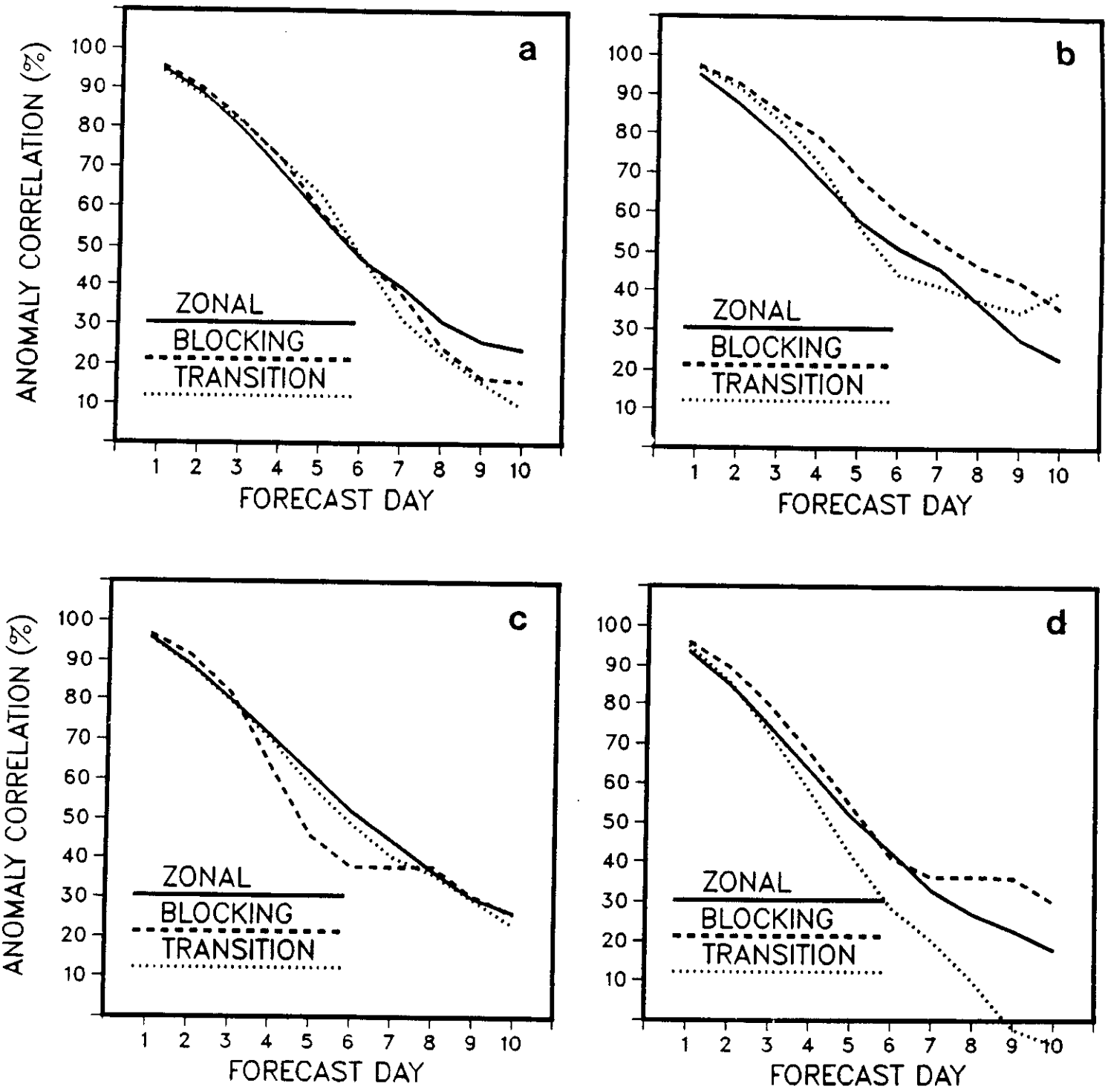
a
b
c
d
ANOMALY CORRELATION (%)
FORECAST DAY
ZONAL
BLOCKING
TRANSITION
100
90
80
70
60
50
40
30
20
10
1 2 3 4 5 6 7 8 9 10

Fig 28